The AI Black-Scholes: Finance-Informed Neural Network

Amine Mohamed Aboussalah[1*], Xuanze Li[2], Cheng Chi[2], Raj Patel[2]

[1*]Department of Finance and Risk Engineering, NYU Tandon School of Engineering, 6 MetroTech Center, Brooklyn, 11201, NY, USA.
[2]Department of Mechanical and Industrial Engineering, University of Toronto, 5 King's College Road, Toronto, M5S 3G8, ON, Canada.

*Corresponding author(s). E-mail(s): ama10288@nyu.edu;

Abstract

In the realm of option pricing, existing models are typically classified into principle-driven methods, such as solving partial differential equations (PDEs) that pricing function satisfies, and data-driven approaches, such as machine learning (ML) techniques that parameterize the pricing function directly. While principle-driven models offer a rigorous theoretical framework, they often rely on unrealistic assumptions, such as asset processes adhering to fixed stochastic differential equations (SDEs). Moreover, they can become computationally intensive, particularly in high-dimensional settings when analytical solutions are not available and thus numerical solutions are needed. In contrast, data-driven models excel in capturing market data trends, but they often lack alignment with core financial principles, raising concerns about interpretability and predictive accuracy, especially when dealing with limited or biased datasets. This work proposes a hybrid approach to address these limitations by integrating the strengths of both principled and data-driven methodologies. Our framework combines the theoretical rigor and interpretability of PDE-based models with the adaptability of machine learning techniques, yielding a more versatile methodology for pricing a broad spectrum of options. We validate our approach across different volatility modeling approaches—both with constant volatility (Black-Scholes) and stochastic volatility (Heston), demonstrating that our proposed framework, Finance-Informed Neural Network (FINN), not only enhances predictive accuracy but also maintains adherence to core financial principles. FINN presents a promising tool for practitioners, offering robust performance across a variety of market conditions.

1 Introduction

In financial mathematics, options represent a fundamental class of derivatives, characterized by their function to provide the right, but not the obligation, for the purchase or sale of an underlying asset at a predetermined price. While this paper primarily employs European options as a test bed for our framework, the methodology we introduce has the potential to be extended to a wider spectrum of options, encompassing both American options and more complex exotic variants.

The significance of options in financial markets extends to hedging, speculative activities, and the broader sphere of risk management. Accurate pricing of options is thus essential, as it aids market participants in assessing risks and rewards, making informed investment decisions, and implementing effective risk management strategies. Various methodologies have been developed for this purpose, falling within the realms of principle-driven and data-driven approaches, each with its own advantages and limitations.

To address the limitations inherent in these traditionally one-sided approaches, our research introduces the Finance-Informed Neural Network (FINN), an integrated method at the intersection of machine learning and financial mathematics for option pricing. To demonstrate how fundamental principles from financial mathematics can be integrated, we directly embed the dynamic hedging principle from the seminal Black-Scholes model derivations into the learning framework. It should be noted that this can be extended to any underlying stochastic model at hand thereby allowing us to leverage the inherent mathematical properties that we would like to preserve. In this work, we transform the mathematical foundations of the Black-Scholes model into neural network loss functions, which serve as training objectives for our machine learning system. This transformation enables our network to learn pricing patterns while inherently respecting no-arbitrage conditions, a financial principle that prevents opportunities for risk-free profits. The learning process operates within a risk-neutral pricing framework, where asset prices are evaluated independently of individual risk preferences, ensuring theoretical consistency with established financial economics. The versatility of FINN is showcased through its adaptability to various underlying stochastic models (geometric Brownian motion & Heston stochastic volatility model). Our framework aims to bridge the gap between principle-driven and data-driven methods, offering a more holistic and robust framework for option pricing. When analytical option pricing solutions are unavailable for complex underlying models, FINN offers a computationally efficient alternative to expensive numerical methods, while preserving essential financial principles including no-arbitrage conditions and dynamic hedging relationships.

In the following sections, we will delve into the Black-Scholes dynamic hedging arguments and demonstrate how we embed it into our proposed FINN framework to enhance option pricing. The primary contributions of this paper are as follows:

1. **Finance-Informed Neural Network (FINN):** We propose a new framework that embeds key financial principles into a neural network architecture. This approach combines the interpretability and theoretical rigor of PDE-based models with the adaptability and data-driven power of neural networks, specifically tailored for option pricing.

2. **Theory-Embedded Neural Network Training:** Our methodology incorporates the No-Arbitrage Principle and dynamic hedging strategies directly into the neural network training process through a carefully constructed loss function. This ensures that the model learns to solve financial derivative pricing problems, maintaining both accuracy and theoretical soundness.

3. **Generalization and Robustness Across Stochastic Processes:** We demonstrate the model's robustness and generalization capabilities by validating its performance across various stochastic processes. Our results show that the model extends effectively from simpler processes, such as geometric Brownian motion, to more sophisticated models like the Heston stochastic volatility model. The framework's generalization capability is demonstrated through accurate estimation of hedge ratios and robust predictive performance across diverse underlying asset dynamics and market conditions.

4. **Generalization of FINN towards Delta-Gamma Hedging:** Beyond traditional delta hedging, our FINN framework demonstrates efficacy in complex hedging strategies, notably delta-gamma hedging. By incorporating established financial hedging theories into its architecture, FINN bridges the gap between computationally expensive numerical methods and neural network approaches, offering enhanced precision and robustness in derivative pricing and risk management applications.

2 Literature review

2.1 Dynamic hedging argument for option pricing

Despite the conceptual simplicity of options, the accurate valuation of European options requires sophisticated mathematical frameworks to address multiple market variables and underlying assumptions. For example, [1] propose the idea of pricing an European option with solving a Partial Differential Equation (PDE) [1], where the option price is composed as a multi-variable function of the underlying stock price (S), option's time-to-maturity (TTM), strike price (K), the underlying stock volatility at the time of pricing (σ) and the risk-free interest rate (r). Solving such a PDE usually requires us to set an initial value and a boundary condition, which are often set according to the option's characteristics such as what happens to the option's value at the maturity date. The value of a call option at expiration is evident: if the strike price (K) exceeds the underlying asset price (S), the option is worthless; If K is less than S, the option's value is $S - K$. A similar logic applies to put options: if K is less than S, the option is worthless; but if K is greater than S, the option's value is $K - S$.

It is worth noting that trading options, like any other financial instrument, comes with inherent risks. Hedging allows traders to mitigate these risks by taking an opposing position in the underlying asset or another related security which can help protect the trader's portfolio against adverse market movements and reduce the overall risk exposure. Delta-hedging is a fundamental risk management strategy that neutralizes portfolio exposure to changes in the underlying asset price. This technique employs the "Delta" - the first-order partial derivative of the option price with respect to the underlying asset price - to determine the optimal offsetting position in the underlying asset. This dynamic hedging approach forms the theoretical foundation of the Black-Scholes partial differential equation and provides a framework for option pricing.

The Black-Scholes PDE emerges through a systematic derivation process: first, by specifying the stochastic dynamics of asset prices; second, by constructing a zero-cost self-financing portfolio; and finally, by imposing no-arbitrage conditions on this portfolio. This sequence of constraints naturally leads to the formulation of the Black-Scholes PDE.

2.1.1 Specification of asset price dynamics

We assume that the underlying asset price follows a Geometric Brownian Motion (GBM). The stochastic differential equation (SDE) is first presented under the real-world probability measure (often called the P-measure):

$$\frac{dS_t}{S_t} = \mu^x dt + \sigma^x dW_t \tag{1}$$

where: S_t represents the asset price at time t, μ^x denotes the expected return (drift) that reflects actual market returns including risk premiums demanded by investors, σ^x represents the asset's volatility, and W_t is a standard Brownian motion (Wiener process). The real-world probability measure describes how asset prices evolve in the actual market, incorporating investors' risk preferences and required risk premiums. This contrasts with the risk-neutral measure used later in pricing, where expected returns are adjusted to the risk-free rate.

The model also requires a riskless bank account, which represents a continuously compounding risk-free investment:

$$\frac{dB_t}{B_t} = rdt \tag{2}$$

This equation describes the growth of one unit of currency invested at the risk-free rate r. It is termed "riskless" because its evolution is deterministic - there is no random component (dW_t term) in its dynamics, making its future values perfectly predictable. While the original Black-Scholes model treats r, μ^x, and σ^x as constants, practical applications require calibrating these parameters using market data.

Consider a derivative security with value g written on the underlying asset S. The price process of this derivative can be represented as $g = (g_t)_{0 < t \leq T}$, where the value at any time t is given by the function $g(t, S_t)$ and the terminal payoff at maturity T is defined by $G(S_T)$.

The stochastic behavior of this derivative can be characterized using Itô's Lemma. Since g_t is a function of both time and the underlying asset price, its stochastic differential equation takes the form:

$$dg_t = \left(\partial_t g + \mu_t^x \partial_x + \frac{1}{2}\left(\sigma_t^x S_t\right)^2 \partial_{xx} g\right) dt + \left(\sigma_t^x S_t \partial_x g\right) dW_t \tag{3}$$

where $\partial_t g$ represents the partial derivative with respect to time, $\partial_x g$ and $\partial_{xx} g$ denote the first and second partial derivatives with respect to the asset price, μ_t^x and σ_t^x are the drift and volatility terms from the underlying asset's process, and dW_t is the Wiener process increment.

This stochastic differential equation, which characterizes the derivative's price dynamics, serves as the key mathematical foundation from which the Black-Scholes PDE emerges.

2.1.2 Construction of zero-cost, self-financing portfolio

Now we construct a zero-cost, self-financing portfolio using the underlying asset S, bank account B and the claim g. Zero-cost means that it costs no money to enter the position specified by the portfolio, and self-financing can be roughly thought of as: any cash outflows for changing the position of one asset are offset by cash inflows from changing the position of another assets within the portfolio. Assume such a portfolio is given by a process $(\alpha, \beta, -1) = (\alpha_t, \beta_t, -1)_{t \geq 0}$ where $\alpha_t, \beta_t, -1$ are the positions we hold at time t on the underlying asset S_t, the bank account B_t and the claim g_t, respectively. We basically take long positions in the underlying asset and the bank account using the money gained from the short position of the contingent claim g that we are trying to price. The corresponding portfolio value process V is given by:

$$V_0 = 0 \quad \text{(zero cost)} \tag{4}$$
$$V_t = \alpha_t S_t + \beta_t B_t - g_t \tag{5}$$
$$dV_t = \alpha_t dS_t + \beta_t dB_t - dg_t \quad \text{(self financing)} \tag{6}$$

We can further expand equation (2.6) by plugging the expressions for dS_t, dB_t and dg_t:

$$dV_t = \alpha_t dS_t + \beta_t dB_t - dg_t = \alpha_t \left(S_t \mu_t^x dt + S_t \sigma_t^x dW_t\right) + \beta_t (r B_t dt) -$$
$$\left(\partial_t g + \mu_t^x S_t \partial_x g + \frac{1}{2}\left(\sigma_t^x S_t\right)^2 \partial_{xx} g\right) dt - \sigma_t^x S_t \partial_x g dW_t = \tag{7}$$
$$\left(\alpha_t S_t \mu_t^x + \beta_t B_t r - \partial_t g - \mu_t^x S_t \partial_x g - \frac{1}{2}(\sigma_t^x S_t)^2 \partial_{xx} g\right) dt + \left(\alpha_t S_t \sigma_t^x - \sigma_t^x S_t \partial_x g\right) dW_t$$

2.1.3 Construction of Zero-Cost, Self-Financing Portfolio

Let us construct a portfolio comprising three components: the underlying asset S, a bank account B, and the derivative g. This portfolio has two key properties:

- Zero-Cost Property: The initial cost to establish the portfolio positions is zero.

- Self-Financing Property: Any changes in portfolio value come solely from asset price changes, not from external cash flows. In other words, the cost of increasing one position is exactly offset by decreasing another position.

The portfolio is defined by the process $(\alpha_t, \beta_t, -1)_{t \geq 0}$, where α_t represents the position in the underlying asset S_t, β_t represents the position in the bank account B_t, and -1 represents a short position in the derivative g_t. The portfolio's value process V is characterized by three key equations:

Initial zero-cost condition:
$$V_0 = 0 \tag{8}$$

Portfolio value at any time t:
$$V_t = \alpha_t S_t + \beta_t B_t - g_t \tag{9}$$

Self-financing condition:
$$dV_t = \alpha_t dS_t + \beta_t dB_t - dg_t \tag{10}$$

Substituting the expressions for dS_t, dB_t, and dg_t into equation (10) yields:

$$dV_t = \alpha_t dS_t + \beta_t dB_t - dg_t = \alpha_t \big(S_t \mu_t^x dt + S_t \sigma_t^x dW_t \big) + \beta_t (r B_t dt) -$$
$$\left(\partial_t g + \mu_t^x S_t \partial_x g + \frac{1}{2} \big(\sigma_t^x S_t \big)^2 \partial_{xx} g \right) dt - \sigma_t^x S_t \partial_x g dW_t = \tag{11}$$
$$\left(\alpha_t S_t \mu_t^x + \beta_t B_t r - \partial_t g - \mu_t^x S_t \partial_x g - \frac{1}{2} (\sigma_t^x S_t)^2 \partial_{xx} g \right) dt + \big(\alpha_t S_t \sigma_t^x - \sigma_t^x S_t \partial_x g \big) dW_t$$

This expanded form separates the deterministic (dt) and stochastic (dW_t) components of the portfolio's value change, providing the basis for deriving no-arbitrage conditions.

2.1.4 Enforcing No-Arbitrage Conditions on the Portfolio

The no-arbitrage principle states that in an efficient market [2], it is impossible to generate risk-free profits without initial investment or taking on any risk. By the no-arbitrage principle, it is impossible for a portfolio to simultaneously satisfy all of the following conditions:

- Requires no initial capital investment (zero-cost)
- Requires no additional capital injection over time (self-financing)
- Has no uncertainty in its value changes (riskless)
- Generates strictly positive returns

Our portfolio already satisfies two conditions: it is zero-cost (8) and self-financing (10). To make it riskless, we eliminate the stochastic component by setting the coefficient of dW_t to zero in Equation (11). This yields the optimal position in the underlying asset:
$$\alpha_t = \partial_x g(t, S_t)$$

The portfolio process becomes $(\partial_x g(t, S_t), \beta_t, -1)_{t \geq 0}$, with its value process described by:

$$V_0 = 0 \tag{12}$$

$$V_t = \partial_x g S_t + \beta_t B_t - g_t \tag{13}$$

$$dV_t = \left(\partial_x g S_t \mu_t^x + \beta_t B_t r - \partial_t g - \mu_t^x S_t \partial_x g - \frac{1}{2} (\sigma_t^x S_t)^2 \partial_{xx} g \right) dt$$
$$= \left(\beta_t B_t r - \partial_t g - \frac{1}{2} (\sigma_t^x S_t)^2 \partial_{xx} g \right) dt \tag{14}$$

To prevent arbitrage in this zero-cost (12), self-financing portfolio (13), riskless (14), the portfolio value must remain constant $dV_t = 0$. Combined with $V_0 = 0$, this implies $V_t = 0$ for all t.

From Equation (13), we obtain $\beta_t = \frac{g_t - \partial_x g S_t}{B_t}$. Substituting this into Equation (14) and setting the dt term to zero yields:

$$\frac{g_t - \partial_x g S_t}{B_t} B_t r - \partial_t g - \frac{1}{2} (\sigma_t^x S_t)^2 \partial_{xx} g = 0$$
$$\partial_t g + \partial_x g S_t r + \frac{1}{2} (\sigma_t^x S_t)^2 \partial_{xx} g = r g_t \tag{15}$$

This equation, combined with the terminal condition $g(T, x) = G(x)$, leads to the Black-Scholes PDE:

$$\left(\partial_t + r \cdot x \cdot \partial_x + \frac{1}{2} (\sigma^x)^2 \cdot x^2 \cdot \partial_{xx} \right) g(t, x) = r \cdot g(t, x)$$
$$g(T, x) = G(x) \tag{16}$$

The Black-Scholes model exhibits two fundamental limitations. First, its assumption of constant volatility contradicts empirical evidence, as market data consistently displays volatility patterns characterized by smiles and skews. Second, the model's reliance on lognormal distribution of asset returns fails to capture important empirical characteristics: market data demonstrates significantly fatter tails and pronounced negative skewness in equity returns, deviating from the model's distributional assumptions. Moreover, there exists fundamental uncertainty about the true underlying distribution of asset returns. These limitations are direct consequences of the model's foundational assumption of Geometric Brownian Motion in Equation (1).

2.2 Machine Learning Approaches to Option Pricing

Machine learning methodologies have fundamentally transformed the landscape of option pricing, offering an alternative paradigm to traditional stochastic calculus

frameworks. These approaches can be broadly classified into two methodological frameworks: direct price prediction and PDE based solutions, each addressing distinct aspects of the option pricing challenge.

The direct price prediction framework originated from early applications of artificial neural networks (ANNs) to price S&P 500 futures options [3]. This study establishes that data-driven approaches provide a robust framework for modeling complex pricing relationships, effectively eliminating the dependency on predefined parametric models. This framework was subsequently enhanced through the incorporation of comprehensive market variables, including the underlying asset price (S_t), strike price (K), time to maturity (τ), dividend yield (q), risk-free interest rate (r), and implied volatility (σ) [4]. This progression led to the emergence of increasingly sophisticated architectures, particularly recurrent neural networks (RNNs) and long short-term memory (LSTM) networks, which explicitly model temporal dependencies in option prices and incorporate non-traditional factors such as market sentiment [5, 6].

The evolution of neural network architectures in option pricing has been marked by increasingly sophisticated approaches to model specification and estimation. Early implementations adopted simple feedforward networks with limited hidden layers to model daily option prices, comparing predictions against traditional benchmarks [7]. Subsequent developments introduced modular approaches, partitioning networks into specialized components based on Moneyness and Time To Maturity (TTM) characteristics to enhance predictive accuracy [8]. These architectures were complemented by methodological advances in uncertainty quantification, notably through the integration of Gaussian Process (GP) models, which provided probabilistic price predictions rather than point estimates [9–11]. These GP-based models overcame the limitations of point-estimate methods, offering richer uncertainty quantification and improved pricing accuracy. Numerous other studies, including [12], [13], [14], and [15] have all further confirmed the robust predictive performance of ANN-driven valuation tools. For an in-depth survey of these developments, we encourage readers to refer to the work of [16] and [17].

Recent research has expanded the methodological frontier through the application of reinforcement learning (RL) techniques, reconceptualizing pricing and hedging as sequential decision-making problems. This approach has enabled the development of adaptive strategies that respond dynamically to changing market conditions [18, 19]. Notably, variants of Q-learning have been employed to develop optimal hedging strategies [20] and the introduction of risk-averse Markov decision processes incorporating time-consistent recursive expectile risk measures [21]. Their actor-critic RL algorithm facilitates the derivation of high-quality, time-consistent hedging policies, while also providing robust option price estimations for complex derivatives, such as basket options. In contrast to static pricing models, these RL-based approaches dynamically adapt strategies in real-time, responding effectively to changing market conditions and evolving risk profiles.

The convergence of these various methodological approaches has established machine learning as a viable complement to traditional option pricing frameworks, offering enhanced flexibility and adaptive capability while maintaining theoretical consistency with established financial principles. The field continues to evolve through the

8

integration of novel architectural designs and learning paradigms, suggesting promising directions for future research in quantitative finance.

The second methodological framework focuses on neural network-based approximations of PDE solutions, leveraging the fundamental relationship between PDEs and SDEs. This approach follows a systematic procedure where we begin with a PDE associated with an underlying asset's SDE, with specified initial conditions. Through the application of Itô's Lemma, we derive an SDE for the state variable from the PDE. This process establishes a Forward-Backward Stochastic Differential Equation (FBSDE) system with known terminal conditions (payoff functions), which can then be solved using various neural network architectures as proposed in recent literature [22–30].

While ML-based approaches offer significant advantages in terms of computational efficiency and adaptability, they face several fundamental challenges that warrant careful consideration. The inherent complexity of neural network architectures often results in black-box systems that lack transparency, presenting significant challenges in risk assessment and management, model validation and verification, and regulatory compliance and auditing. Furthermore, pure data-driven approaches may fail to incorporate fundamental financial principles, potentially leading to violations of no-arbitrage conditions, inconsistent pricing across related derivatives, and departures from put-call parity relationships.

The effectiveness of ML models in option pricing fundamentally depends on the data used to train them, much like how a student's learning depends on the quality of their study materials. These models face three key data-related challenges. First, when certain market scenarios occur rarely in the training data (imagine having very few examples of extreme market conditions), the model's predictions become less reliable in these situations. Second, if historical data contains persistent patterns that don't reflect current market reality (similar to learning from outdated textbooks), the model may perpetuate these outdated patterns in its predictions. Third, the model may struggle when encountering market conditions that differ significantly from its training examples - just as someone might struggle to apply concepts to entirely new situations. These challenges suggest that a better approach would be to combine machine learning's ability to learn from data with the fundamental principles from traditional financial models, creating a balance between empirical learning and theoretical foundations.

This paper introduces FINN (Finance-Informed Neural Network), a new neural network framework for option pricing that makes three key contributions. First, FINN explicitly incorporates fundamental financial constraints into its architecture, embedding financial theories, such as no-arbitrage principles, directly into the learning process. This addresses the theoretical consistency limitations inherent in traditional ML approaches. Second, we made multiple runs and computed the average and standard deviation, enabling robust model assessment and risk management with clearly defined confidence levels across varying market conditions. Third, we develop an interpretable architecture that maintains pricing consistency across related instruments,

9

enhancing real-world applicability. Our empirical results demonstrate that FINN successfully bridges the gap between data-driven learning and financial theory, delivering both accurate and theoretically sound pricing predictions.

3 Finance-Informed Neural Network (FINN)

Our Finance-Informed Neural Network (FINN) is a framework that integrates fundamental financial principles with deep learning architecture for option pricing. This section details how we transform traditional financial theory into a practical machine learning framework while preserving essential pricing principles. At its core, FINN embeds the dynamic hedging arguments and no-arbitrage principles detailed in Section 2.1 directly into the neural network's learning process. Rather than treating these principles as external constraints, we transform them into training objectives that guide the network's learning. This ensures that our model learns to price options in a way that inherently respects financial theory.

The key idea of our work lies in our parameterization of the option pricing function. We replace the traditional pricing process g_t with a neural network function g_t^θ, where θ represents the network parameters. This function takes as input a feature set I_t containing relevant market variables (such as current stock price S_t, strike price K, and time to maturity) and outputs option prices $g_t^\theta(I_t)$. Importantly, we leverage modern deep learning frameworks' auto-differentiation capabilities to compute the derivative terms $(\partial_x g^\theta)$ that are essential for implementing dynamic hedging strategies.

Our approach differs from traditional methods in its treatment of the underlying asset price process. Instead of assuming a specific model like Geometric Brownian Motion (GBM), we allow for flexibility in the data source. The price process can be informed by various stochastic models or real market data, making our framework more adaptable to different market conditions. We approximate the term dS_t using finite difference methods, while the neural network provides the necessary derivative terms through auto-differentiation.

The fundamental contribution of our approach is the transformation of the no-arbitrage principle into a neural network training objective. In traditional theory, this principle leads to the condition $dV_t = 0$ for the portfolio value process. We reformulate this condition into a loss function that guides the training of our neural network g^θ. This approach ensures that our model learns to generate option prices that respect fundamental financial principles while maintaining the flexibility to adapt to complex market dynamics. Through this integration of financial theory and machine learning, FINN provides a theoretically sound yet practically implementable framework for option pricing.

Detailed FINN Methodology. Our Finance-Informed Neural Network (FINN) methodology integrates dynamic hedging principles with neural network architecture through a systematic approach. At its foundation lies the portfolio value process, expressed as:

$$dV_t = \alpha_t dS_t + \beta_t dB_t - dg_t^\theta(I_t) \tag{17}$$

where g^θ represents our neural network's option pricing function, taking input features I_t at time t. To maintain the fundamental properties of a riskless, zero-cost, self-financing portfolio, we define the portfolio positions as $\alpha_t = \partial_x g_t$ and $\beta_t = \frac{g_t - \partial_x g S_t}{B_t}$, with the bank account return $\frac{dB_t}{B_t} = r_t dt$. This formulation ensures the portfolio value remains constant:

$$dV_t = \partial_x g_t^\theta(I_t)dS_t + r_t\big(g_t^\theta(I_t) - \partial_x g_t^\theta(I_t)S_t\big)dt - dg_t^\theta(I_t) = 0 \qquad (18)$$

A significant feature of our approach is the translation of this financial principle into a neural network training objective. We calculate $\partial_x g_t^\theta(I_t)$ through automatic differentiation, while market data provides r_t, S_t, dS_t, and I_t. The term $dg_t^\theta(I_t)$ is approximated using finite differences with sequential inputs I_t, I_{t+1}, and I_{t-1}. This leads to our training loss function:

$$\text{loss} = \Big(\underbrace{\partial_x g_t^\theta(I_t)}_{\text{Delta }(\Delta)} dS_t + r_t(g_t^\theta(I_t) - \underbrace{\partial_x g_t^\theta(I_t)}_{\text{Delta }(\Delta)} S_t)dt - dg_t^\theta(I_t)\Big)^2 \qquad (19)$$

Our framework extends naturally to incorporate additional Greeks beyond Delta (Δ). Since Greeks represent derivatives of the pricing function with respect to various inputs, we can compute them using the same automatic differentiation techniques. This enables us to construct similar loss functions for more complex hedging strategies, such as Delta-Gamma neutral pricing. For enhanced risk management through Delta-Gamma hedging, we further incorporate a hedging instrument (typically another option with different characteristics) into our portfolio alongside the primary option we are pricing. This results in a portfolio with four components, represented by the positions $(\alpha_t, \beta_t, \eta_t, -1)$, where α_t is the position in the underlying asset, β_t is the position in the risk-free bank account, η_t is the position in the hedging instrument, and -1 represents the short position in the option we are pricing. This approach allows us to neutralize both first-order (Delta) and second-order (Gamma) price risks simultaneously, providing more comprehensive protection against price movements in the underlying asset. For more details, we refer the reader to Section 5.5. This extension follows similar principles to those outlined earlier, with all terms expressible through either auto-differentiation or market data. This unified approach allows us to train a single neural network to learn no-arbitrage pricing functions directly from market data.

It is worth noting that while our approach uses expressions similar to those in Itô processes, we make no specific assumptions about drift and volatility functions. Unlike traditional methods that require explicit modeling of these functions, FINN learns them implicitly during training. This represents a significant advantage: we preserve the rigorous structure of dynamic hedging arguments while eliminating restrictive assumptions about the underlying price process. The following Theorem 1 establishes the convergence properties of the FINN model under delta-gamma hedging constraints in a self-supervised learning framework. It provides rigorous guarantees for approximating the arbitrage-free price and its derivatives. The detailed proof of this theorem is presented in the Appendix A.2.

11

Theorem 1 (FINN Convergence under Delta-Gamma Hedging). *Let g^θ be a FINN model parameterized by θ, trained via a self-supervised approach on data generated from a complete, arbitrage-free market with underlying asset S_t and additional instrument(s) H_t. Assume:*

1. *The loss function $\mathcal{L}$ incorporates delta-gamma hedging constraints and is derived solely from the underlying stochastic process and the associated PDE conditions, without external supervised labels.*
2. *The market is free of arbitrage and complete, ensuring a unique equivalent martingale measure $\mathbb{Q}$ and a unique arbitrage-free price g^*.*
3. *The neural network has sufficient capacity (universal approximation property in suitable function spaces, including the approximation of first and second spatial derivatives).*

Then, for any $\epsilon > 0$, there exists a set of parameters θ^* such that:

$$\sup_{t, S_t, H_t} |g^\theta(S_t, H_t) - g^*(S_t, H_t)| < \epsilon,$$

$$|\Delta_{g^\theta}(t, S_t, H_t) - \Delta_g(t, S_t, H_t)| < \epsilon, \quad |\Gamma_{g^\theta}(t, S_t, H_t) - \Gamma_g(t, S_t, H_t)| < \epsilon,$$

where $\Delta_g = \partial_S g^*$ and $\Gamma_g = \partial_S^2 g^*$ are the first and second derivatives with respect to the underlying asset price S_t.

4 Experimental Setup

This section details our experimental methodology for evaluating FINN's option pricing capabilities across different underlying asset models. We present a systematic approach to training and testing our model, following the design illustrated in Figure 1.
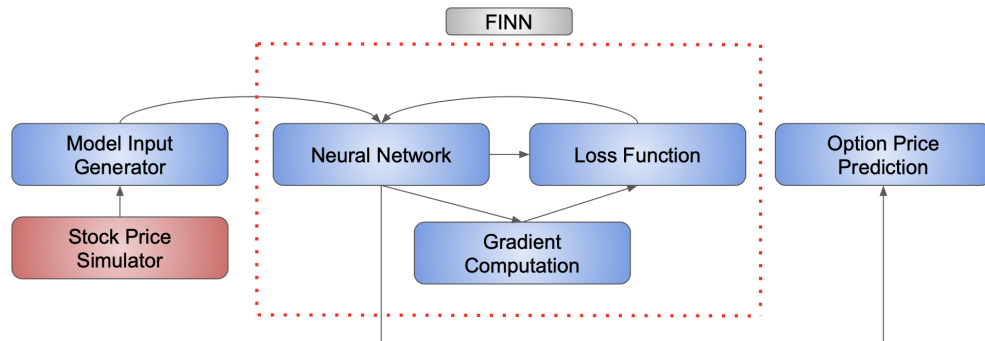
Fig. 1: Overview of the FINN Model Design

The training process consists of three primary components. First, we employ a Stock Price Simulator, which generates synthetic price paths based on predefined

SDEs. We specifically test our pricing methodology using two distinct models: the Geometric Brownian Motion (GBM) and the Heston stochastic volatility model (detailed specifications provided in the Appendix A.3 and A.4). These models represent different levels of complexity in asset price dynamics, allowing us to assess FINN's adaptability.

Second, our Model Input Generator transforms the simulated price paths into structured training data. This process involves dividing the price paths into temporal batches and augmenting each data point with randomly assigned strike prices (K) and times to maturity (T). This approach ensures our training data covers a diverse range of option characteristics, enhancing the model's ability to generalize across different market conditions.

Third, we implement the training procedure itself. FINN processes each batch through a forward pass, generating option price predictions that are evaluated using the dynamic hedging loss function detailed in Algorithm 1. The resulting loss guides the optimization of the model's parameters through backpropagation. To prevent overfitting, we employ an early stopping mechanism based on a held-out validation dataset.

For model evaluation, we follow a similar but distinct process. We generate new price paths from the same underlying SDEs used in training, ensuring our test scenarios reflect the intended market dynamics. The Model Input Generator then creates test cases that systematically vary specific option parameters while holding others constant. For instance, to evaluate strike price sensitivity, we generate options with varying strikes while maintaining consistent maturity and other characteristics. This allows us to assess FINN's pricing accuracy across different option specifications. Model performance is evaluated by comparing FINN's predictions against analytical solutions (for GBM) or established numerical methods such as Monte Carlo simulation (for Heston). Comprehensive results from these experiments are presented in Section 5.

This experimental framework enables us to rigorously evaluate FINN's ability to learn and apply fundamental pricing principles across different market conditions and option specifications.

Algorithm 1 FINN - Delta & Gamma Hedging for Vanilla European Options

---

Require: S_t: underlying asset price at time t, K: strike price, T: time to maturity, S_{t+1}: underlying asset price at time $t+1$, r: risk-free rate, `option_type`: either 'call' or 'put', C_{ATM}: option price for at-the-money option, Δ_{ATM}: delta sensitivity for at-the-money (ATM) option, Γ_{ATM}: gamma sensitivity for at-the-money (ATM) option

1: **Step 1: Compute Inputs for the Neural Network**
2: $\quad X_t \leftarrow \left(\frac{S_t}{K \cdot \exp(-r \cdot T)}, T \right)$
3: $\quad X_{t+1} \leftarrow \left(\frac{S_{t+1}}{K \cdot \exp(-r \cdot (T-1))}, T-1 \right)$
4: **Step 2: Estimate Option Prices at t and $t+1$**
5: **if** `option_type == 'call'` **then**
6: $\quad C_t \leftarrow K \cdot \exp(-r \cdot T) \cdot \max \left(\frac{S_t}{K \cdot \exp(-r \cdot T)} - 1, 0 \right)$
7: $\quad C_{t+1} \leftarrow K \cdot \exp(-r \cdot (T-1)) \cdot \max \left(\frac{S_{t+1}}{K \cdot \exp(-r \cdot (T-1))} - 1, 0 \right)$
8: **else if** `option_type == 'put'` **then**
9: $\quad C_t \leftarrow K \cdot \exp(-r \cdot T) \cdot \max \left(1 - \frac{S_t}{K \cdot \exp(-r \cdot T)}, 0 \right)$
10: $\quad C_{t+1} \leftarrow K \cdot \exp(-r \cdot (T-1)) \cdot \max \left(1 - \frac{S_{t+1}}{K \cdot \exp(-r \cdot (T-1))}, 0 \right)$
11: **end if**
12: **Step 3: Compute Sensitivities (Delta and Gamma)**
13: $\quad \Delta, \Gamma \leftarrow$ compute gradient of C_t w.r.t. S_t
14: $\quad$ Bound Δ and Γ within $[0, 1]$
15: **Step 4: Hedging Strategy**
16: $\quad$ **(a) If Delta Hedging**
17: $\quad\quad V_t \leftarrow -C_t + \Delta \cdot S_t$
18: $\quad\quad V_{t+1} \leftarrow -C_{t+1} + \Delta \cdot S_{t+1}$
19: $\quad$ **(b) If Delta & Gamma Hedging**
20: $\quad\quad \beta \leftarrow \frac{\Gamma}{\Gamma_{\text{ATM}}}$
21: $\quad\quad \alpha \leftarrow \Delta - \beta \cdot \Delta_{\text{ATM}}$
22: $\quad\quad V_t \leftarrow -C_t + \alpha \cdot S_t + \beta \cdot C_{\text{ATM}}$
23: $\quad\quad V_{t+1} \leftarrow -C_{t+1} + \alpha \cdot S_{t+1} + \beta \cdot C_{\text{ATM}_{t+1}}$
24: **Step 5: Minimize the Hedging Error**
25: $\quad$ Minimize Mean Squared Error(V_t, V_{t+1})

---

5 Results and Discussion

5.1 Numerical Example: FINN Implementation with GBM

To illustrate FINN's practical implementation, let us consider a simple example using a two-layer neural network to price a European call option under Geometric Brownian Motion (Appendix A.3) . We will demonstrate how FINN computes and minimizes the delta-hedging loss.

Initial Market Conditions:
- Current stock price (S_t): $120
- Strike price (K): $100
- Risk-free rate (r): 0%
- Time to maturity (τ): 0.24 years

Consider a scenario where the stock price increases by 1 unit, such that $S_{t+1} = \$121$. Our FINN model, denoted as g^θ, takes as input I_t which includes:

- Price ratio ($\frac{S_t}{K}$)
- Time to maturity (τ)

Let's demonstrate the loss calculation process:

Delta Computation:
FINN estimates a hedge ratio $\Delta = \partial_S g_t^\theta(I_t) = 0.5$. The change in stock position value:
$\Delta \cdot (S_{t+1} - S_t) = 0.5 \cdot (121 - 120) = 0.5$

Option Price Change:
- FINN output at time t: $g_t^\theta(I_t) = 10$
- FINN output at time $t+1$: $g_{t+1}^\theta(I_{t+1}) = 11$
- Change in option value: $g_{t+1}^\theta(I_{t+1}) - g_t^\theta(I_t) = 1$

Delta-Hedging Loss:
Loss $= [\Delta \cdot (S_{t+1} - S_t) - (g_{t+1}^\theta(I_{t+1}) - g_t^\theta(I_t))]^2 = [0.5 - (11 - 10)]^2 = 0.16$

The model then uses TensorFlow's mean squared error optimization to minimize this hedging discrepancy:

$$\mathcal{L} = \mathbb{E}[(\Delta \cdot (S_{t+1} - S_t) - (g_{t+1}^\theta(I_{t+1}) - g_t^\theta(I_t)))^2] \tag{20}$$

This example demonstrates how FINN combines financial principles (delta hedging) with machine learning optimization to improve option pricing accuracy.

In Figure 2, we illustrate the simple example discussed earlier using a 2-period framework. At time $t + 1$, the stock price can evolve in one of two directions: it can either increase or decrease, resulting in two possible scenarios for the option price. Specifically, the option price can remain at 11 or decrease to 9. The loss for the objective function is then computed as the difference between the change in the stock portfolio value and the change in the FINN model's output for the option price.
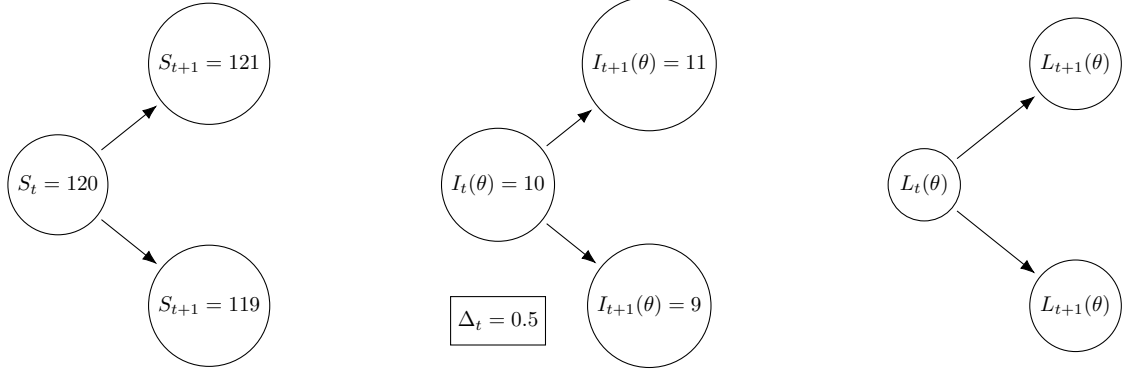
$$L_\theta(t) = \sqrt{(S_{t+1} - S_t) \cdot \Delta_t - (I_{t+1}(\theta) - I_t(\theta))^2}$$

Fig. 2: A one-period illustrative example

To validate our approach, we compare FINN's predictions with the Black-Scholes model using a trained neural network with the following architecture:

Structure:

- Two hidden layers, each containing 50 neurons
- Output layer producing normalized option prices ($\frac{C}{K}$)
- Softmax activation in the output layer

The network takes a two-dimensional input vector x:

$$x = \begin{bmatrix} \frac{S}{K} \\ T \end{bmatrix} \tag{21}$$

where $\frac{S}{K}$ represents the normalized spot price and T is time to maturity. The first layer transformation, with weights $W^{[1]}$ and biases $b^{[1]}$, can be represented as:

$$W^{[1]} = \begin{bmatrix} w_{1,1}^{[1]} & w_{1,2}^{[1]} \\ w_{2,1}^{[1]} & w_{2,2}^{[1]} \\ \vdots & \vdots \\ w_{50,1}^{[1]} & w_{50,2}^{[1]} \end{bmatrix}, \qquad b^{[1]} = \begin{bmatrix} b_1^{[1]} \\ b_2^{[1]} \\ \vdots \\ b_{50}^{[1]} \end{bmatrix} \qquad a^{[1]} = f^{[1]}\left(W^{[1]}x + b^{[1]}\right)$$

16

The first layer applies the hyperbolic tangent (tanh) activation function to its linear transformation:

$$a^{[1]} = \tanh(W^{[1]}x + b^{[1]}) \in \mathbb{R}^{50} \tag{22}$$

where $a^{[1]}$ represents the vector of 50 activations from the first layer. These activations then serve as input to the second layer, with weights $W^{[2]} \in \mathbb{R}^{50 \times 50}$ and biases $b^{[2]} \in \mathbb{R}^{50}$:

$$a^{[2]} = \tanh(W^{[2]}a^{[1]} + b^{[2]}) \tag{23}$$

$$W^{[2]} = \begin{bmatrix} w_{1,1}^{[2]} & w_{1,2}^{[2]} & \cdots & w_{1,50}^{[2]} \\ w_{2,1}^{[2]} & w_{2,2}^{[2]} & \cdots & w_{2,50}^{[2]} \\ \vdots & \vdots & \ddots & \vdots \\ w_{50,1}^{[2]} & w_{50,2}^{[2]} & \cdots & w_{50,50}^{[2]} \end{bmatrix}, \quad b^{[2]} = \begin{bmatrix} b_1^{[2]} \\ b_2^{[2]} \\ \vdots \\ b_{50}^{[2]} \end{bmatrix}$$

The final layer transforms the second layer's activations into the normalized option price $\frac{C}{K}$ using a softplus activation function. The output layer's parameters are:

$$W^{[3]} = \begin{bmatrix} w_{11}^{[3]} & w_{12}^{[3]} & \cdots & w_{150}^{[3]} \end{bmatrix} \in \mathbb{R}^{1 \times 50}, \quad b^{[3]} \in \mathbb{R} \tag{24}$$

The final output is computed as:

$$\frac{C}{K} = \text{softplus}(W^{[3]}a^{[2]} + b^{[3]}) = \ln(1 + e^{W^{[3]}a^{[2]} + b^{[3]}}) \tag{25}$$

5.2 Training Example and Numerical Implementation

We demonstrate FINN's practical implementation using a neural network trained over 250 epochs under the following conditions:

- Geometric Brownian Motion environment
- Volatility (σ): 0.125
- Initial stock price (S_0): \$100

To validate our trained network's performance, we examine an in-the-money European call option with the following characteristics:

- Moneyness ratio ($\frac{S}{K}$): 1.1 (indicating the option is 10% in-the-money)
- Time to maturity: 0.36 years (approximately 90 days)

The network's predicted option prices are compared against the analytical Black-Scholes solutions, demonstrating the model's ability to learn the theoretical pricing relationship. This example input vector is represented as:

$$x = \begin{bmatrix} \frac{S}{K} & \text{TTM} \end{bmatrix} = \begin{bmatrix} 1.1 & 0.36 \end{bmatrix} \tag{26}$$

17

The first layer's parameters after training are:

$$W^{[1]} = \begin{bmatrix} -0.374 & 0.131 \\ -0.514 & 0.110 \\ -0.506 & 0.360 \\ \vdots & \vdots \\ 0.195 & -0.793 \\ -0.587 & -1.470 \end{bmatrix} \in \mathbb{R}^{50 \times 2}, \quad b^{[1]} = \begin{bmatrix} -0.0161 \\ 0.3584 \\ 0.3024 \\ \vdots \\ 0.0571 \\ 0.4862 \end{bmatrix} \in \mathbb{R}^{50} \qquad (27)$$

For our example input:

$$x = \begin{bmatrix} 1.1 & 0.36 \end{bmatrix} \qquad (28)$$

The first layer's activation is computed as:

$$a^{[1]} = \tanh(W^{[1]}x + b^{[1]}) \qquad (29)$$

Explicitly:

$$a^{[1]} = \tanh\left(\begin{bmatrix} -0.374 & 0.131 \\ -0.514 & 0.110 \\ -0.506 & 0.360 \\ \vdots & \vdots \\ 0.195 & -0.793 \\ -0.587 & -1.470 \end{bmatrix} \begin{bmatrix} 1.1 \\ 0.36 \end{bmatrix} + \begin{bmatrix} -0.0161 \\ 0.3584 \\ 0.3024 \\ \vdots \\ 0.0571 \\ 0.4862 \end{bmatrix} \right) \qquad (30)$$

The first layer's activation $a^{[1]} \in \mathbb{R}^{50}$ is computed as:

$$a^{[1]} = \begin{bmatrix} -0.3633 \\ -0.1659 \\ -0.1242 \\ \vdots \\ -0.0137 \\ -0.5970 \end{bmatrix} \qquad (31)$$

For the second layer transformation, with parameters:

$$W^{[2]} = \begin{bmatrix} -0.364 & -0.158 & -0.227 & \cdots & 0.139 & -0.324 \\ 0.182 & 1.045 & 0.458 & \cdots & -0.468 & 0.960 \\ -0.091 & -0.046 & 0.099 & \cdots & 0.164 & 0.275 \\ \vdots & \vdots & \vdots & \ddots & \vdots & \vdots \\ -0.435 & -0.370 & -0.320 & \cdots & 0.357 & -0.390 \\ 0.395 & 0.165 & 0.373 & \cdots & -0.017 & 0.407 \end{bmatrix} \in \mathbb{R}^{50 \times 50} \qquad (32)$$

18

$$b^{[2]} = \begin{bmatrix} 0.248 \\ 0.183 \\ 0.090 \\ \vdots \\ 0.085 \\ -0.990 \end{bmatrix} \in \mathbb{R}^{50} \tag{33}$$

The second layer's activation is:

$$a^{[2]} = \tanh(W^{[2]}a^{[1]} + b^{[2]}) = \begin{bmatrix} 0.9999 \\ -0.9920 \\ -0.1724 \\ \vdots \\ -0.9999 \\ -0.9999 \end{bmatrix} \tag{34}$$

The output layer parameters are:

$$W^{[3]} = \begin{bmatrix} -0.372 & -0.221 & -0.327 & \cdots & 0.726 & 0.280 \end{bmatrix} \in \mathbb{R}^{1\times50}, \quad b^{[3]} = [-0.0965] \tag{35}$$

The final normalized option price is computed as:

$$\frac{C}{K} = \text{softplus}(W^{[3]}a^{[2]} + b^{[3]}) = \text{softplus}(0.1039) = 0.1039 \tag{36}$$

Our trained FINN model generates results that closely align with the Black-Scholes model's theoretical values. Specifically, for our example option, FINN produces a price of \$10.39 (computed as $0.1039 \times K = 0.1039 \times 100$), which differs by only \$0.01 from the Black-Scholes price of \$10.38. Similarly, FINN's estimated Delta of 0.86, obtained through automatic differentiation, approximates the Black-Scholes Delta of 0.90 with reasonable accuracy. These results demonstrate FINN's capability to learn both accurate option prices and their corresponding hedge ratios, effectively replicating the Black-Scholes model's pricing and risk metrics through a neural network framework.

5.3 Results for Geometric Brownian Motion

We present a comprehensive evaluation of FINN using simulated data where the underlying asset follows geometric Brownian motion (GBM). The analysis focuses on European call options under various market conditions to demonstrate the model's robustness and accuracy.

Experimental Design

The evaluation framework encompasses the following parameters:
  Option Characteristics:

- Maturity Range: 60-120 days (medium-term options)
- Stock Price (S): Sample space of 10,000 points ranging from \$75 to \$125

- Strike Price (K): Range from \$90 to \$110, with \$1 increments
- Volatility (σ): Multiple scenarios from 0.125 to 0.175
- Annual Return (α): 6% (inflation-adjusted real-world return)
- Dividend Yield: 0% (non-dividend-paying underlying)

Evaluation Methodology

Our analysis employs both visual and statistical approaches to assess FINN's performance:

1. Visual Comparison:

   - FINN Predictions: Represented by red curves
   - Theoretical Values: Black-Scholes solutions shown in green curves
   - Deviation Analysis: Secondary plots showing the difference between FINN predictions and Black-Scholes values

2. Statistical Analysis: We conduct extensive testing with:

   - Number of Independent Runs: 10
   - Different Random Seeds: 10 per run
   - Key Metrics: Mean Absolute Deviation (MAD) and Mean Squared Error (MSE)

   These metrics evaluate two crucial aspects:

   1. Option Price Accuracy: Comparing predicted prices against Black-Scholes values
   2. Hedge Ratio Precision: Assessing the accuracy of computed Delta values

Results Documentation

The comprehensive performance metrics are documented in Table 1, which presents:

- Average MAD and MSE across all runs
- Standard deviations of error metrics
- Performance breakdown by volatility scenario

This rigorous evaluation framework allows us to assess FINN's capability in replicating both the pricing and hedging aspects of the Black-Scholes model across diverse market conditions.

Our comprehensive empirical analysis validates FINN's effectiveness in option pricing and hedging applications. The model demonstrates remarkable precision, with average pricing deviations below 0.2 (less than 1%) for options priced up to 35, while maintaining consistently low hedge ratio deviations of approximately 0.01 (see Table 1). Our investigation reveals important relationships between market parameters and model performance. Specifically, we observe that higher underlying stock volatility correlates with increased prediction deviation, reflecting the inherent complexity of pricing options on more volatile assets. Additionally, the Time to Maturity (TTM) influences model accuracy, with shorter-term options generally yielding lower Mean Absolute Deviation (MAD) and Mean Squared Error (MSE), likely due to their simpler pricing dynamics. The model's robustness is further demonstrated through parallel experiments with put options, which yield comparable accuracy to call options

Table 1: FINN Testing Results on Various Volatility Levels, TTMs, and Strikes (GBM) for Call Options. Results are averaged across strikes from 75 to 125, based on 10,000 data points, with the final values being averaged over 10 independent runs, the values in bracket are the standard deviation.

| Vol σ	TTM τ	Call Option Price (C) Estimation				Hedge Ratio (Δ) Estimation			
		MAD		MSE		MAD		MSE	
	0.24	0.164	(0.037)	0.051	(0.023)	0.021	(0.005)	0.001	(0.000)
	0.28	0.175	(0.040)	0.057	(0.026)	0.022	(0.005)	0.001	(0.000)
	0.32	0.184	(0.043)	0.062	(0.028)	0.023	(0.005)	0.001	(0.000)
0.125	0.36	0.191	(0.046)	0.066	(0.031)	0.023	(0.005)	0.001	(0.000)
	0.40	0.196	(0.049)	0.068	(0.033)	0.023	(0.005)	0.001	(0.000)
	0.44	0.199	(0.051)	0.069	(0.034)	0.022	(0.005)	0.001	(0.000)
	0.48	0.200	(0.053)	0.069	(0.035)	0.022	(0.005)	0.001	(0.000)
	0.24	0.218	(0.048)	0.085	(0.037)	0.026	(0.006)	0.001	(0.000)
	0.28	0.234	(0.053)	0.095	(0.042)	0.026	(0.006)	0.001	(0.000)
	0.32	0.246	(0.057)	0.102	(0.046)	0.026	(0.006)	0.001	(0.000)
0.15	0.36	0.254	(0.060)	0.107	(0.050)	0.027	(0.006)	0.001	(0.000)
	0.40	0.259	(0.064)	0.110	(0.052)	0.026	(0.006)	0.001	(0.000)
	0.44	0.262	(0.067)	0.110	(0.054)	0.026	(0.006)	0.001	(0.000)
	0.48	0.262	(0.070)	0.109	(0.055)	0.025	(0.006)	0.001	(0.000)
	0.24	0.282	(0.066)	0.132	(0.056)	0.030	(0.006)	0.001	(0.001)
	0.28	0.301	(0.071)	0.146	(0.063)	0.030	(0.007)	0.001	(0.001)
	0.32	0.315	(0.076)	0.156	(0.069)	0.031	(0.007)	0.001	(0.001)
0.175	0.36	0.326	(0.081)	0.164	(0.074)	0.031	(0.007)	0.001	(0.001)
	0.40	0.333	(0.084)	0.168	(0.077)	0.030	(0.007)	0.001	(0.001)
	0.44	0.336	(0.088)	0.169	(0.080)	0.030	(0.007)	0.001	(0.001)
	0.48	0.336	(0.091)	0.167	(0.082)	0.029	(0.007)	0.001	(0.000)

(detailed results available in Appendix A.5, Figure A1 and Table A1). These consistent results across different option types and market conditions, even when using synthetic data, underscore FINN's reliability as a comprehensive tool for option pricing and hedging applications. Figure 3 provides an illustrative comparison of call option price and hedge ratio estimations obtained from testing FINN on a 2-month Time to Maturity (TTM) call option. The stock prices are simulated using a Geometric Brownian Motion model with a volatility of 15%.
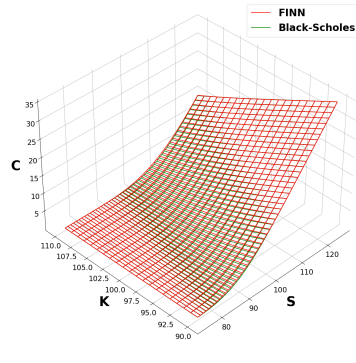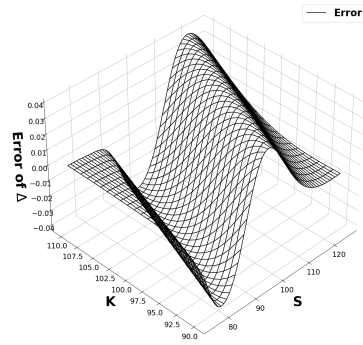
(a) Estimated Call Option Price for Given S and K
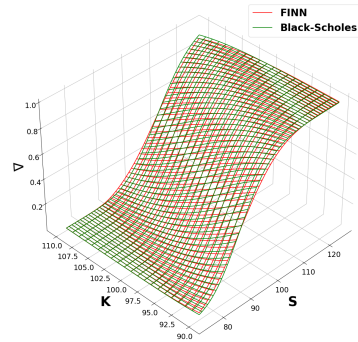
(b) Estimated Hedge Ratio (Δ) Given S and K
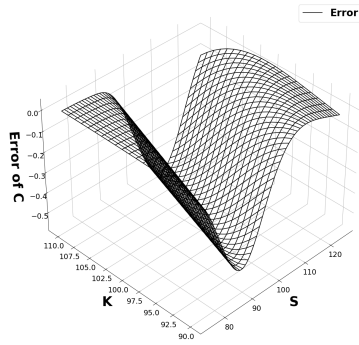
(c) Error of Predicted Call Price

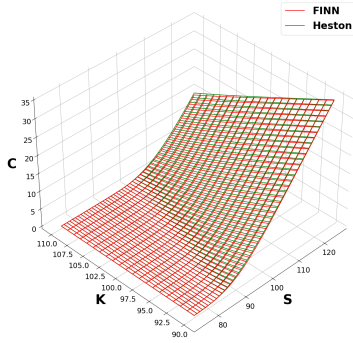(d) Error of Predicted Hedge Ratio (Δ)

Fig. 3: Comparison of Call Option Prices, Hedge Ratios, and Errors

## 5.4 Performance Analysis Under Heston Stochastic Volatility Model

Following our evaluation methodology from the GBM analysis, we examine FINN's performance under the Heston stochastic volatility framework. We conduct experiments across three volatility of volatility (VolVol) scenarios: 0.125, 0.150, and 0.175, with ten independent runs per scenario to ensure statistical significance. The results are summarized in Table 2 below.

Table 2: FINN Testing Results on Various Volatility Levels, TTMs, and Strikes (Heston) for Call Options. Results are averaged across strikes from 75 to 125, based on 10,000 data points, with the final values being averaged over 10 independent runs, the values in bracket are the standard deviation.

VolVol ξ	TTM τ	Call Option Price (C) Estimation MAD		MSE		Hedge Ratio (Δ) Estimation MAD		MSE	
	0.24	0.238	(0.137)	0.117	(0.123)	0.027	(0.017)	0.001	(0.001)
	0.28	0.263	(0.144)	0.137	(0.138)	0.029	(0.017)	0.002	(0.002)
	0.32	0.286	(0.150)	0.156	(0.152)	0.030	(0.017)	0.002	(0.002)
0.125	0.36	0.307	(0.154)	0.174	(0.164)	0.031	(0.017)	0.002	(0.002)
	0.40	0.326	(0.157)	0.191	(0.173)	0.032	(0.017)	0.002	(0.002)
	0.44	0.344	(0.158)	0.206	(0.180)	0.033	(0.017)	0.002	(0.002)
	0.48	0.359	(0.159)	0.221	(0.185)	0.033	(0.017)	0.002	(0.001)
	0.24	0.247	(0.124)	0.125	(0.120)	0.029	(0.015)	0.002	(0.001)
	0.28	0.272	(0.137)	0.147	(0.138)	0.030	(0.015)	0.002	(0.001)
	0.32	0.294	(0.148)	0.168	(0.155)	0.032	(0.015)	0.002	(0.001)
0.15	0.36	0.315	(0.156)	0.188	(0.169)	0.033	(0.016)	0.002	(0.002)
	0.40	0.334	(0.163)	0.205	(0.180)	0.034	(0.016)	0.002	(0.002)
	0.44	0.351	(0.168)	0.222	(0.190)	0.035	(0.015)	0.002	(0.002)
	0.48	0.367	(0.171)	0.237	(0.197)	0.035	(0.015)	0.002	(0.001)
	0.24	0.266	(0.121)	0.149	(0.142)	0.031	(0.013)	0.002	(0.001)
	0.28	0.297	(0.131)	0.176	(0.162)	0.033	(0.013)	0.002	(0.001)
	0.32	0.327	(0.139)	0.204	(0.181)	0.034	(0.013)	0.002	(0.001)
0.175	0.36	0.354	(0.145)	0.232	(0.198)	0.036	(0.013)	0.002	(0.001)
	0.40	0.379	(0.150)	0.258	(0.212)	0.037	(0.013)	0.002	(0.001)
	0.44	0.402	(0.154)	0.284	(0.223)	0.038	(0.013)	0.002	(0.001)
	0.48	0.423	(0.157)	0.308	(0.233)	0.039	(0.013)	0.002	(0.001)

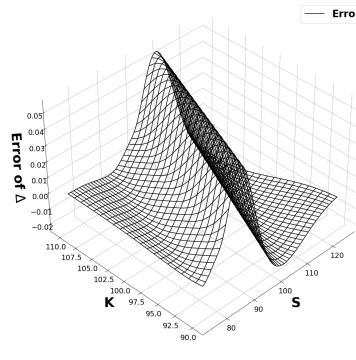(a) Estimated Call Option Price for Given S and K (Heston)
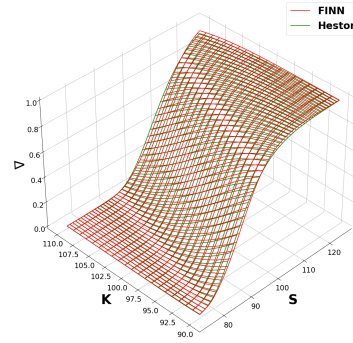
(b) Estimated Hedge Ratio (Δ) Given S and K (Heston)
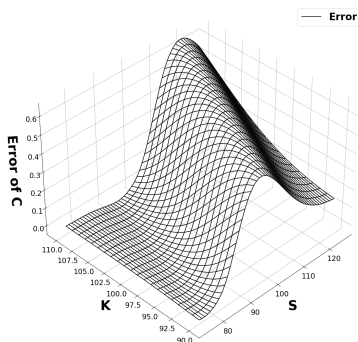
(c) Error of Predicted Call Price (Heston)

(d) Error of Predicted Hedge Ratio (Δ) (Heston)

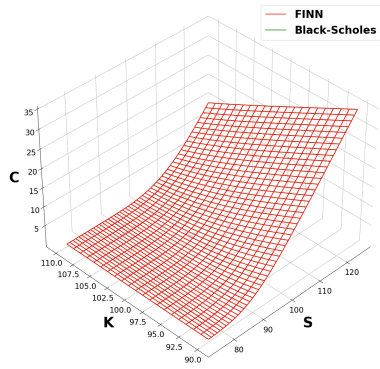**Fig. 4**: Comparison of Call Option Prices, Hedge Ratios, and Errors (Heston Model)

Our empirical analysis demonstrates FINN's robust capability in approximating both option prices and hedge ratios within the Heston framework. The model achieves significant pricing accuracy, maintaining average deviations below 0.4 (less than 2%) for options valued up to 40. Similarly, hedge ratio estimations exhibit consistent precision with average deviations of approximately 0.03, validating FINN's reliability for risk management applications. Figure 4 presents a comparison of FINN's performance against the Heston analytical solutions. The test is conducted under conditions of 15% volatility of volatility to price a 2-month Time to Maturity (TTM) call option, with stock prices simulated using the Heston stochastic volatility model.

A key finding emerges from the relationship between model performance and market parameters. The volatility of volatility parameter demonstrates a notable impact on prediction accuracy, where higher VolVol values correlate with increased prediction deviations. This relationship aligns with the theoretical understanding that increased stochastic volatility complexity leads to more challenging option pricing scenarios. Additionally, we observe that TTM influences model accuracy, with shorter-term options generally yielding Mean Absolute Deviation (MAD) and Mean Squared Error (MSE), reflecting reduced complexity in near-term option pricing. To validate FINN's versatility, we extend our analysis to put options, conducting parallel experiments that yield comparable results detailed in Figure A2, Table A2 (Appendix A.6). This consistency across option types reinforces FINN's robustness in capturing the complex dynamics of the Heston model, demonstrating its effectiveness as a comprehensive option pricing and hedging tool under stochastic volatility conditions.

5.5 Delta-Gamma Risk Management through Enhanced FINN Framework

We extend FINN's capabilities to incorporate both delta and gamma risk management through the introduction of a hedging instrument in the portfolio construction. This enhancement, implemented through Algorithm 1, enables simultaneous neutralization of first-order and second-order price risks. The modification requires expanding our loss function to achieve both delta and gamma neutrality, resulting in a more comprehensive risk management framework. Our empirical validation employs a 30-day at-the-money (ATM) option as the hedging instrument, where both the hedging option and the target option share the same underlying stochastic process. The results, documented in Table A3 (Appendix A.7), demonstrate substantial improvements over traditional delta-only hedging strategies. Notably, at a volatility level of 0.125, the Mean Absolute Deviation (MAD) in option price estimation decreases significantly from 0.164 (delta hedging) to 0.024 (delta-gamma hedging). This pattern of improvement persists across various volatility levels, validating the enhanced accuracy achieved through gamma risk incorporation. Figure 5 illustrates FINN's accurate estimations of option prices, hedge ratios, and option gamma under a volatility level of 0.15, a 2-month time to maturity, and a 30-day hedging period. The underlying stock prices are simulated using a Geometric Brownian Motion model. To assess the robustness of our enhanced framework, we conducted additional experiments varying the time to maturity (TTM) of the hedging instrument. The results demonstrate consistent performance improvements across different TTM configurations, including tests with a

90-day hedging option. This consistency in error reduction spans all evaluated metrics - option prices, delta values, and gamma values - providing strong empirical support for our theory-embedded, self-supervised approach. These findings indicate that the incorporation of gamma hedging not only enhances pricing accuracy but also significantly improves the model's capacity to learn and generalize option sensitivities (Greeks), thereby offering a more comprehensive solution for option pricing and risk management.
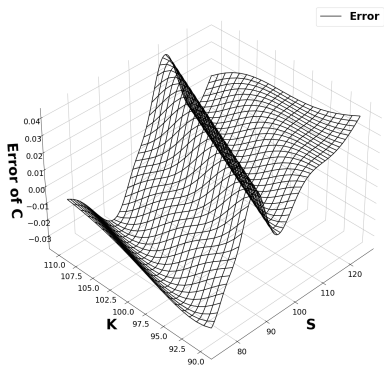
(a) Estimated Call Option Price for Given S and K
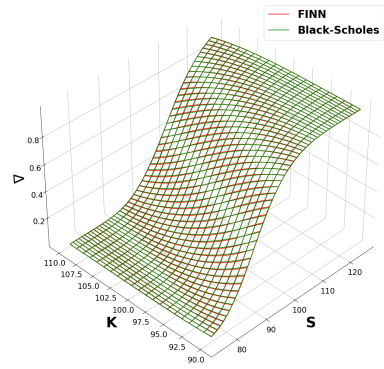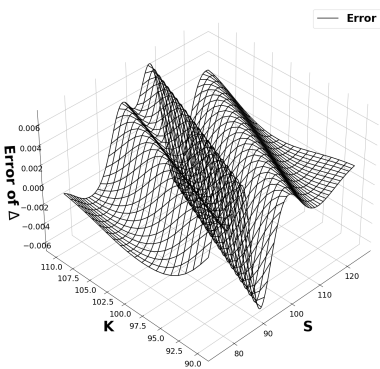

(b) Estimated Hedge Ratio (Δ) Given S and K
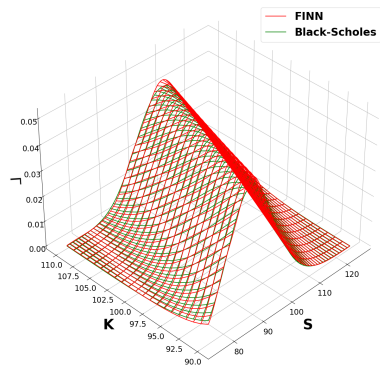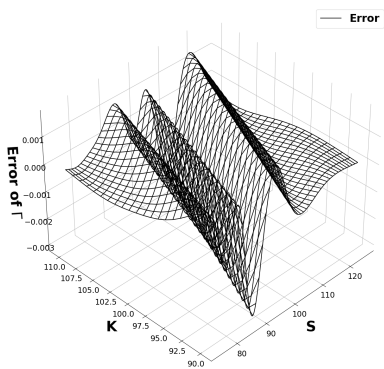

(c) Estimated Option Gamma (Γ) Given S and K

(d) Error of Predicted Call Price

(e) Error of Predicted Hedge Ratio (Δ)

26

(f) Error of Predicted Option Gamma (Γ)

Fig. 5: Comparison of Call Option Prices, Hedge Ratios, Gamma, and Errors

6 Conclusion and Future Directions

This research advances the field of option pricing by introducing the Finance-Informed Neural Network (FINN), a new framework that synthesizes fundamental financial principles with modern machine learning approaches. By embedding hedging principles directly into the neural network architecture through carefully designed loss functions, FINN maintains theoretical consistency while leveraging the computational advantages of machine learning. Our empirical results validate FINN's effectiveness across multiple pricing frameworks, from the classical Black-Scholes to the more complex Heston stochastic volatility model, demonstrating high accuracy in both option pricing and Greeks estimation. The incorporation of delta-gamma hedging further demonstrates FINN's capability to capture complex market dynamics and provide comprehensive risk management solutions, significantly improving upon traditional delta-only hedging approaches.

Despite these achievements, several promising research directions warrant further investigation. Future work could explore the implementation of probabilistic learning frameworks such as Gaussian Processes or Bayesian Neural Networks, and extend the application to exotic options with discontinuous payoff functions. Additionally, the integration of vega risk hedging in complex stochastic volatility models presents an important avenue for development. Theoretical extensions could include multi-asset options and complex derivatives, investigation of model behavior under extreme market conditions, and development of adaptive learning mechanisms for changing market dynamics.

FINN's success in combining theoretical principles with machine learning capabilities suggests a promising direction for financial modeling beyond option pricing, potentially extending to other areas of quantitative finance where theoretical constraints must be balanced with empirical data. The methodologies developed in this research provide a foundation for future innovations in financial modeling, particularly in scenarios where traditional analytical solutions are intractable or computational efficiency is paramount. As financial markets continue to evolve in complexity, approaches like FINN that maintain theoretical rigor while embracing computational advances will become increasingly valuable. The adaptability and precision of our framework demonstrate its potential to transform option pricing and hedging strategies across a wide range of market conditions and scenarios, establishing a robust foundation for future financial models and practices.

References

[1] Black, F., Scholes, M.: The pricing of options and corporate liabilities. Journal of Political Economy **81**(3), 637–654 (1973)

[2] Varian, H.R.: The arbitrage principle in financial economics. Journal of Economic Perspectives **1**(2), 55–72 (1987)

[3] Hutchinson, J., Lo, A., Poggio, T.: A nonparametric approach to pricing and hedging derivative securities via learning networks. Journal of Finance **49**(3), 851–889 (1994)

[4] Culkin, R., Das, S.: Machine learning in finance: the case of deep learning for option pricing. Journal of Investment Management **15**, 92–100 (2017)

[5] Xie, H., You, T.: Research on european stock index option pricing based on deep learning algorithms–evidence from 50etf option market. Statistics Information Forum **33**, 99–106 (2018). (in Chinese)

[6] Ke, C.: A study of option price prediction based on lstm neural network. Master's thesis, Southeast University (2021). (in Chinese)

[7] Amilon, H.: A neural network versus black-scholes: A comparison of pricing and hedging performances. Journal of Forecasting **22**(4), 317–335 (2003)

[8] Gradojevic, N., Gençay, R., Kukolj, D.: Option pricing with modular neural networks. IEEE Transactions on Neural Networks **20**(4), 626–637 (2009)

[9] Han, G.-S., Lee, J.: Prediction of pricing and hedging errors for equity linked warrants with gaussian process models. Expert Systems with Applications **35**(1), 515–523 (2008)

[10] Yang, S.-H., Lee, J.: Predicting a distribution of implied volatilities for option pricing. Expert Systems with Applications **38**(3), 1702–1708 (2011)

[11] Park, H., Lee, J.: Forecasting nonnegative option price distributions using bayesian kernel methods. Expert Systems with Applications **39**(18), 13243–13252 (2012)

[12] Anders, U., Korn, O., Schmitt, C.: Improving the pricing of options: A neural network approach. Journal of Forecasting **17**(5–6), 369–388 (1998)

[13] Garcia, R., Gençay, R.: Pricing and hedging derivative securities with neural networks and a homogeneity hint. Journal of Econometrics **94**(1), 93–115 (2000)

[14] Yao, J., Li, Y., Tan, C.L.: Option price forecasting using neural networks. Omega **28**(4), 455–466 (2000)

[15] Liu, S., Oosterlee, C.W., Bohte, S.M.: Pricing options and computing implied volatilities using neural networks. Risks **7**(1), 1–22 (2019)

[16] Park, H., Kim, N., Lee, J.: Parametric models and non-parametric machine learning models for predicting option prices: Empirical comparison study over kospi

200 index options. Expert Systems with Applications **41**(11), 5227–5237 (2014)

[17] Ivașcu, C.-F.: Option pricing using machine learning. Expert Systems with Applications **163**, 113799 (2021)

[18] Grassl, T.: A reinforcement learning approach for pricing derivatives. The Stanford Encyclopedia of Philosophy (2010)

[19] Martín, K.: Reinforcement learning applied to option pricing. Master's thesis, University of the Witwatersrand, Faculty of Science (2014)

[20] Halperin, I.: Qlbs: Q-learner in the black-scholes(-merton) worlds. arXiv preprint arXiv:1712.04609 (2019)

[21] Marzban, S., Delage, E., Li, J.Y.-M.: Deep reinforcement learning for option pricing and hedging under dynamic expectile risk measures. Quantitative Finance **23**(10), 1411–1430 (2023)

[22] Karniadakis, G., Kevrekidis, I., Lu, L., Perdikaris, P., Wang, S., Yang, L.: Physics-informed machine learning. Nature Reviews Physics **3**, 422–440 (2021)

[23] Raissi, M., Perdikaris, P., Karniadakis, G.: Physics-informed neural networks: A deep learning framework for solving forward and inverse problems involving nonlinear partial differential equations. Journal of Computational Physics **378**, 686–707 (2019)

[24] Höök, L., Ludvigsson, G., Sydow, L.: The kolmogorov forward fractional partial differential equation for the cgmy-process with applications in option pricing. Computers & Mathematics with Applications **76**, 2330–2344 (2018)

[25] Patel, R., Hsing, C., Sahin, S., Jahromi, S., Palmer, S., Sharma, S., Michel, C., Porte, V., Abid, M., Aubert, S., Castellani, P., Lee, C., Mugel, S., Orus, R.: Quantum-inspired tensor neural networks for partial differential equations (2022)

[26] Patel, R., Hsing, C., Sahin, S., Palmer, S., Jahromi, S., Sharma, S., Dominguez, T., Tziritas, K., Michel, C., Porte, V., Abid, M., Aubert, S., Castellani, P., Mugel, S., Orus, R.: Quantum-inspired tensor neural networks for option pricing (2022)

[27] Patel, R., Dominguez, T., Dib, M., Palmer, S., Cadarso, A., Contreras, F., Ratnani, A., Casanova, F., Hernandez-Santana, S., Diaz-Fernandez, A., Andres, E., Luis-Hita, J., Sanchez-Martinez, E., Mugel, S., Orus, R.: Application of tensor neural networks to pricing bermudan swaptions (2023)

[28] E, W., Han, J., Jentzen, A.: Deep learning-based numerical methods for high-dimensional parabolic partial differential equations and backward stochastic differential equations. Communications in Mathematics and Statistics **5**, 349–380 (2017)

[29] Beck, C., Arnold, A., Criens, D., Schwab, C., Zimmer, J.: Solving stochastic differential equations and kolmogorov equations by means of deep learning. arXiv preprint arXiv:1806.00421 (2018)

[30] Han, J., Jentzen, A., E., W.: Solving high-dimensional partial differential equations using deep learning. PNAS **115**, 8505–8510 (2018)

[31] Hull, J.: Options, Futures, and Other Derivatives. Pearson, Boston :Prentice Hall (2018)

[32] Delbaen, F., Schachermayer, W.: A general version of the fundamental theorem of asset pricing. Mathematische Annalen **300**(1), 463–520 (1994)

[33] Harrison, J.M., Pliska, S.R.: Martingales and stochastic integrals in the theory of continuous trading. Stochastic Processes and Their Applications **11**(3), 215–260 (1981)

[34] Karatzas, I., Shreve, S.E.: Methods of Mathematical Finance. Springer, New York (1998)

[35] Friedman, A.: Stochastic Differential Equations and Applications. Academic Press, New York (1975)

[36] Goodfellow, I., Bengio, Y., Courville, A.: Deep Learning. MIT Press, Cambridge, MA (2016)

[37] Rudin, W.: Principles of Mathematical Analysis, 3rd edn. McGraw-Hill, New York (1976). International Edition

[38] Vom Scheidt, J.: Review of *Numerical Solution of Stochastic Differential Equations* by Kloeden, P. E. and Platen, E. ZAMM - Journal of Applied Mathematics and Mechanics / Zeitschrift für Angewandte Mathematik und Mechanik. Springer-Verlag, Berlin etc., 1992. XXXVI, 632 pp., 85 figs., DM 118, OO. (1994)

[39] Heston, S.L.: A closed-form solution for options with stochastic volatility with applications to bond and currency options. The Review of Financial Studies **6**(2), 327–343 (1993)

[40] Cox, J.C., Ingersoll, J.E., Ross, S.A.: A theory of the term structure of interest rates. Econometrica **53**(2), 385–407 (1985)

[41] Albrecher, H., Mayer, P., Schoutens, W., Tistaert, J.: The little heston trap. Wilmott Magazine, 83–92 (2007)

Appendix A

A.1   Overview of Options

In financial world, an option is a financial instrument giving the holder the right, without obligation, to buy or sell an underlying asset (S) at a predetermined strike price (K). It is one particular class of financial derivatives, whose values are generally derived from another underlying processes or assets. A call option gives the holder the right but not the obligation to buy the underlying asset at the strike price, while a put option gives the holder the right to sell the underlying asset at the strike price. Options can be classified into different types, with European and American being the most common. European options are those which have a specific expiration date, while American options typically have a validity period during which they can be exercised at any time. Options that don't fit into either category are called "exotic options". This paper primarily focuses on the simple scenario - the European options, which the only exercise date for the option holders is at expiration.

Options are widely used for hedging, speculation, and risk management in financial markets [31]. Therefore, option pricing becomes a crucial aspect of financial decision-making, as it enables market participants to assess the potential risks and rewards associated with option contracts. Accurate pricing helps in making informed investment decisions, evaluating the profitability of potential trades, and implementing risk management strategies. It allows investors and traders to determine whether an option is overvalued or undervalued in relation to the prevailing market conditions, aiding in the identification of potential opportunities for buying or selling options. Various methodologies have been developed for accurately pricing options.

A.2   Theoretical Properties

Proof of the Theorem

Theorem 2 (FINN Convergence under Delta-Gamma Hedging). *Let g^θ be a FINN model parameterized by θ, trained via a self-supervised approach on data generated from a complete, arbitrage-free market with underlying asset S_t and additional instrument(s) H_t. Assume:*

1. *The loss function $\mathcal{L}$ incorporates delta-gamma hedging constraints and is derived solely from the underlying stochastic process and the associated PDE conditions, without external supervised labels.*
2. *The market is free of arbitrage and complete, ensuring a unique equivalent martingale measure $\mathbb{Q}$ and a unique arbitrage-free price g^*.*
3. *The neural network has sufficient capacity (universal approximation property in suitable function spaces, including the approximation of first and second spatial derivatives).*

Then, for any $\epsilon > 0$, there exists a set of parameters θ^* such that:

$$\sup_{t, S_t, H_t} |g^\theta(S_t, H_t) - g^*(S_t, H_t)| < \epsilon,$$

31

$$|\Delta_{g^\theta}(t, S_t, H_t) - \Delta_g(t, S_t, H_t)| < \epsilon, \quad |\Gamma_{g^\theta}(t, S_t, H_t) - \Gamma_g(t, S_t, H_t)| < \epsilon,$$

where $\Delta_g = \partial_S g^*$ and $\Gamma_g = \partial_S^2 g^*$ are the first and second derivatives with respect to the underlying asset price S_t.

Proof. **Part I: Existence of the True Pricing Function g^*.**

Definition 1 (Market Setting). *Let $(\Omega, \mathcal{F}, (\mathcal{F}_t)_{0 \leq t \leq T}, \mathbb{P})$ be a filtered probability space satisfying the usual conditions, where $T < \infty$ represents the time horizon. Consider a financial market with:*

- *An underlying asset price process $(S_t)_{0 \leq t \leq T}$*
- *A hedging instrument price process $(H_t)_{0 \leq t \leq T}$*
- *A risk-free rate process $(r_t)_{0 \leq t \leq T}$*

Assumption 1 (Market Properties). *The market satisfies:*

1. *Completeness: All contingent claims are replicable*
2. *No arbitrage: There exist no trading strategies yielding risk-free profits*
3. *Regularity: All price processes are continuous semimartingales*

Theorem 3 (Existence and uniqueness of Pricing Function). *Under Assumption 1, there exists a unique equivalent martingale measure $\mathbb{Q} \sim \mathbb{P}$ and a unique pricing function $g^* : [0, T] \times \mathbb{R}_+ \times \mathbb{R} \to \mathbb{R}$ such that for any contingent claim with terminal payoff $f(S_T, H_T)$:*

$$g^*(t, S_t, H_t) = \mathbb{E}^{\mathbb{Q}}\left[e^{-\int_t^T r_s ds} f(S_T, H_T) \mid \mathcal{F}_t\right] \tag{A1}$$

Proof. The proof follows from the Fundamental Theorem of Asset Pricing (FTAP) in continuous time.

(I) - Existence of Equivalent Martingale Measure:
Under Assumption 1, specifically the no-arbitrage condition, by the FTAP (see Delbaen and Schachermayer [32]), there exists at least one equivalent local martingale measure $\mathbb{Q} \sim \mathbb{P}$ such that the discounted price processes

$$\tilde{S}_t = e^{-\int_0^t r_s ds} S_t \quad \text{and} \quad \tilde{H}_t = e^{-\int_0^t r_s ds} H_t \tag{A2}$$

are local martingales under $\mathbb{Q}$.

(II) - Uniqueness of Martingale Measure:
By the market completeness assumption in Assumption 1, every derivative contract is replicable. Therefore, by Harrison and Pliska [33], the equivalent martingale measure $\mathbb{Q}$ is unique.

(III) - Construction of Pricing Function:
Define the pricing function $g^* : [0, T] \times \mathbb{R}_+ \times \mathbb{R} \to \mathbb{R}$ as:

$$g^*(t, S_t, H_t) = \mathbb{E}^{\mathbb{Q}}\left[e^{-\int_t^T r_s ds} f(S_T, H_T) \mid \mathcal{F}_t\right] \tag{A3}$$

(IV) - Uniqueness of Pricing Function:
The uniqueness of g^* follows from:

1. The uniqueness of $\mathbb{Q}$ (from (II))
2. The martingale representation theorem in complete markets
3. The law of iterated expectations

Specifically, if there were another pricing function $\hat{g}$, their difference would create an arbitrage opportunity, contradicting Assumption 1.

The detailed technical arguments can be found in Delbaen and Schachermayer [32] for (I), Harrison and Pliska [33] for (II) and (IV), Karatzas and Shreve [34] for (III) $\quad\square$

Proposition 4 (PDE Characterization). *The function g^* is the unique classical solution to the backward parabolic PDE:*

$$\begin{cases} \partial_t g^* + \mathcal{L}^{\mathbb{Q}} g^* - r_t g^* = 0 & in \ [0,T] \times \mathbb{R}_+ \times \mathbb{R} \\ g^*(T,s,h) = f(s,h) & on \ \{T\} \times \mathbb{R}_+ \times \mathbb{R} \end{cases} \tag{A4}$$

where $\mathcal{L}^{\mathbb{Q}}$ is the infinitesimal generator of (S_t, H_t) under $\mathbb{Q}$.

Assumption 2 (Regularity Conditions). *Assume:*

1. *The coefficients of $\mathcal{L}^{\mathbb{Q}}$ are continuous and bounded*
2. *The operator $\mathcal{L}^{\mathbb{Q}}$ is uniformly elliptic*
3. *The payoff function f is continuous and has polynomial growth*

Theorem 5 (Regularity of Solution). *Under Assumption 2, the solution g^* to (A4) satisfies:*

1. *$g^* \in C^{1,2}([0,T] \times \mathbb{R}_+ \times \mathbb{R})$*
2. *The Greeks $\Delta_g = \partial_s g^*$ and $\Gamma_g = \partial_s^2 g^*$ exist and are continuous*
3. *g^* and its derivatives have polynomial growth*

Proof. The regularity follows from classical PDE theory for parabolic equations under the given assumptions. For details, see [35] or [34]. $\quad\square$

Part II: FINN: A Self-Supervised Learning Framework

Definition 2 (Neural Network Parameterization). *Let $g^\theta : [0,T] \times \mathbb{R}_+ \to \mathbb{R}$ be a neural network with parameters $\theta \in \Theta$, where Θ is a compact subset of $\mathbb{R}^d$. For fixed strike price K, the network takes inputs:*

$$x = (S/K, T-t) \in \mathbb{R}_+ \times [0,T] \tag{A5}$$

and outputs the normalized price $g^\theta(x)$.

Definition 3 (Delta-Hedging Loss Function). *The delta-hedging loss $\mathcal{L}_\Delta : \Theta \to \mathbb{R}_+$ is defined as:*

$$\mathcal{L}_\Delta(\theta) = \mathbb{E}\left[\left(\partial_s g_t^\theta(I_t)dS_t + r_t(g_t^\theta(I_t) - \partial_s g_t^\theta(I_t)S_t)dt - dg_t^\theta(I_t)\right)^2\right] \tag{A6}$$

where $\partial_s g_t^\theta$ represents the network's approximation of the delta hedge ratio.

Definition 4 (Delta-Gamma Hedging Loss Function). *The delta-gamma hedging loss*
$\mathcal{L}_{\Delta,\Gamma} : \Theta \to \mathbb{R}_+$ *is defined as:*

$$\mathcal{L}_{\Delta,\Gamma}(\theta) = \mathcal{L}_\Delta(\theta) + \lambda \mathbb{E}\left[(\partial_s^2 g_t^\theta(I_t) - \Gamma_g(t, S_t, H_t))^2\right] \tag{A7}$$

where $\lambda > 0$ is a weighting parameter.

Theorem 6 (Self-Supervised Learning Properties). *Under appropriate regularity*
conditions, the following properties hold:

1. If g^θ satisfies $\mathcal{L}_\Delta(\theta) = 0$, then g^θ satisfies the no-arbitrage PDE.
2. If $\mathcal{L}_{\Delta,\Gamma}(\theta) = 0$, then g^θ additionally satisfies second-order hedging constraints.

Proof. (I) - Analysis of Delta-Hedging Loss
Suppose $\mathcal{L}_\Delta(\theta) = 0$. This implies almost surely:

$$\partial_s g_t^\theta(I_t)dS_t + r_t(g_t^\theta(I_t) - \partial_s g_t^\theta(I_t)S_t)dt = dg_t^\theta(I_t) \tag{A8}$$

(II) - Application of Itô's Formula
By Itô's formula, the right-hand side expands to:

$$dg_t^\theta(I_t) = \partial_t g^\theta dt + \partial_s g^\theta dS_t + \frac{1}{2}\partial_s^2 g^\theta (dS_t)^2 \tag{A9}$$

Under $\mathbb{Q}$, the underlying follows:

$$dS_t = r_t S_t dt + \sigma_t S_t dW_t^{\mathbb{Q}} \tag{A10}$$

Therefore, $(dS_t)^2 = \sigma_t^2 S_t^2 dt$ (in quadratic variation).
(III) - Equating Terms
Substituting these expressions and matching coefficients of dt and $dW_t^{\mathbb{Q}}$:

$$dt : \partial_t g^\theta + \frac{1}{2}\sigma_t^2 S_t^2 \partial_s^2 g^\theta + r_t S_t \partial_s g^\theta - r_t g^\theta = 0 \tag{A11}$$

$$dW_t^{\mathbb{Q}} : \text{terms cancel} \tag{A12}$$

This is precisely the no-arbitrage PDE.
(IV) - Analysis of Delta-Gamma Loss
When $\mathcal{L}_{\Delta,\Gamma}(\theta) = 0$, we additionally have:

$$\partial_s^2 g_t^\theta(I_t) = \Gamma_g(t, S_t, H_t) \tag{A13}$$

By the results from Steps (I)-(III) and this additional constraint, g^θ satisfies both:

1. The no-arbitrage PDE (from $\mathcal{L}_\Delta(\theta) = 0$)
2. The second-order hedging constraint (from the Γ term)

The regularity of these solutions follows from classical results in stochastic calculus (see Karatzas and Shreve [34]) and the smoothness of neural networks with respect to their inputs. $\square$

Proposition 7 (PDE-Driven Curvature Learning). *The network learns the correct second derivatives through three mechanisms:*

1. *PDE-Implicit Constraints: The solution space is restricted by:*

$$\partial_t g^\theta + \mathcal{L}^{\mathbb{Q}} g^\theta - r_t g^\theta = 0 \qquad (A14)$$

2. *Self-Consistency: For any $\theta \in \Theta$, the PDE residual:*

$$R(\theta) = \|\partial_t g^\theta + \mathcal{L}^{\mathbb{Q}} g^\theta - r_t g^\theta\|_{L^2} \qquad (A15)$$

   provides a natural error metric.
3. *Automatic Differentiation: The derivatives $\partial_s g^\theta$ and $\partial_s^2 g^\theta$ are computed explicitly through the network architecture.*

Proof. We prove this proposition by demonstrating how each mechanism contributes to learning the correct second derivatives.

(I) - PDE-Implicit Constraints

Let g^θ be a neural network solution. The PDE constraint implies:

$$\partial_s^2 g^\theta = -\frac{2}{\sigma^2 S^2} \left(\partial_t g^\theta + rS \partial_s g^\theta - r g^\theta \right) \qquad (A16)$$

This provides an implicit characterization of $\partial_s^2 g^\theta$ in terms of other derivatives and the function value.

(II) - Self-Consistency Analysis

For the L^2 residual:

$$R(\theta) = \left\| \partial_t g^\theta + \frac{1}{2} \sigma^2 S^2 \partial_s^2 g^\theta + rS \partial_s g^\theta - r g^\theta \right\|_{L^2} \qquad (A17)$$

By the Sobolev embedding theorem, for sufficiently smooth g^θ:

$$\|g^\theta\|_{W^{2,2}} \leq C(1 + R(\theta)) \qquad (A18)$$

for some constant $C > 0$. This bounds the L^2 norm of second derivatives.

(III) - Automatic Differentiation Implementation

The neural network g^θ can be written as a composition:

$$g^\theta = \phi_L \circ \phi_{L-1} \circ ... \circ \phi_1 \qquad (A19)$$

35

where each ϕ_i is differentiable. By the chain rule:

$$\partial_s g^\theta = \sum_{i=1}^{L} \frac{\partial \phi_L}{\partial \phi_i} \frac{\partial \phi_i}{\partial s} \tag{A20}$$

$$\partial_s^2 g^\theta = \sum_{i,j=1}^{L} \frac{\partial^2 \phi_L}{\partial \phi_i \partial \phi_j} \frac{\partial \phi_i}{\partial s} \frac{\partial \phi_j}{\partial s} + \sum_{i=1}^{L} \frac{\partial \phi_L}{\partial \phi_i} \frac{\partial^2 \phi_i}{\partial s^2} \tag{A21}$$

These derivatives are computed exactly through backpropagation (see Goodfellow et al. [36]).

(IV) - Convergence

The combination of these mechanisms ensures:

1. PDE constraints provide the target form for $\partial_s^2 g^\theta$
2. Residual minimization enforces consistency
3. Exact computation allows gradient-based optimization

Therefore, as $R(\theta) \to 0$, the network learns the correct second derivatives. $\qquad\square$

Part III: Universal Approximation of the Pricing Solution and Its Derivatives.

Since g^* is unique and sufficiently smooth, and g^θ is represented by a neural network with suitable activation functions (e.g., smooth, non-polynomial), known results from approximation theory imply that neural networks can approximate g^* arbitrarily well. Moreover, neural networks can approximate not only functions but also their derivatives to arbitrary precision on compact sets, provided g^* is in an appropriate Sobolev space.

Sobolev Space Framework and Neural Network Approximation Properties:

In order to establish a rigorous analytical setting for assessing the smoothness and approximation properties of the pricing function, we introduce an appropriate functional framework grounded in Sobolev spaces.

Definition 5 (Domain of Analysis). *Let $D \subset \mathbb{R}^3$ be the compact set defined as*

$$D := [0, T] \times [S_{\min}, S_{\max}] \times [H_{\min}, H_{\max}] \tag{A22}$$

equipped with the standard Euclidean topology.

Definition 6 (Sobolev Space). *For $k \in \mathbb{N}$ and domain D, we define the Sobolev space $W^{k,\infty}(D)$ as*

$$W^{k,\infty}(D) := g \in L^\infty(D) : \partial^\alpha g \in L^\infty(D) \text{ for all } |\alpha| \leq k \tag{A23}$$

where $\alpha = (\alpha_1, \alpha_2, \alpha_3)$ is a multi-index with $|\alpha| = \alpha_1 + \alpha_2 + \alpha_3$.

Proposition 8 (Norm Structure). *The space $W^{k,\infty}(D)$ is a Banach space when equipped with the norm*

$$|g|_{W^{k,\infty}(D)} := \max_{|\alpha| \leq k} |\partial^\alpha g|_{L^\infty(D)} \tag{A24}$$

where $\partial^\alpha g$ denotes the mixed partial derivative

$$\partial^\alpha g := \frac{\partial^{|\alpha|} g}{\partial t^{\alpha_1} \partial s^{\alpha_2} \partial h^{\alpha_3}} \tag{A25}$$

Lemma 9 (Regularity of the Pricing Function). *Under Assumptions 1-3, the pricing function g^* belongs to $W^{2,\infty}(D)$.*

Theorem 10 (Neural Network Approximation). *Let $\sigma : \mathbb{R} \to \mathbb{R}$ be a smooth activation function. For any $\epsilon > 0$, there exists a neural network architecture with parameters θ_ϵ such that*

$$|g^{\theta_\epsilon} - g^*|_{W^{2,\infty}(D)} < \epsilon \tag{A26}$$

Corollary 10.1 (Uniform Convergence of Derivatives). *The approximation in $W^{2,\infty}(D)$ implies uniform convergence of the function and its derivatives up to order 2:*

$$\sup_{x \in D} |g^{\theta_\epsilon}(x) - g^*(x)| < \epsilon \tag{A27}$$

$$\sup_{x \in D} |\partial_s g^{\theta_\epsilon}(x) - \partial_s g^*(x)| < \epsilon \tag{A28}$$

$$\sup_{x \in D} |\partial_s^2 g^{\theta_\epsilon}(x) - \partial_s^2 g^*(x)| < \epsilon \tag{A29}$$

where $x := (t, s, h)$.

Proof. Let us prove this result step by step. First, recall that by definition of the $W^{2,\infty}(D)$ norm:

$$|g^{\theta_\epsilon} - g^*|_{W^{2,\infty}(D)} = \max_{|\alpha| \leq 2} |\partial^\alpha(g^{\theta_\epsilon} - g^*)|_{L^\infty(D)} < \epsilon \tag{A30}$$

For any multi-index α with $|\alpha| \leq 2$, we have:

$$|\partial^\alpha(g^{\theta_\epsilon} - g^*)|_{L^\infty(D)} \leq \max_{|\beta| \leq 2} |\partial^\beta(g^{\theta_\epsilon} - g^*)|_{L^\infty(D)} = |g^{\theta_\epsilon} - g^*|_{W^{2,\infty}(D)} < \epsilon \tag{A31}$$

By the definition of the L^∞ norm:

$$|\partial^\alpha(g^{\theta_\epsilon} - g^*)|_{L^\infty(D)} = \operatorname*{ess\,sup}_{x \in D} |\partial^\alpha(g^{\theta_\epsilon} - g^*)(x)| \tag{A32}$$

37

The essential supremum is used instead of the regular supremum because L^∞ functions might be undefined or infinite on a set of measure zero. Since g^{θ_ϵ} and g^* are smooth functions (by construction and assumption respectively), the essential supremum coincides with the supremum:

$$\operatorname*{ess\,sup}_{x \in D} |\partial^\alpha (g^{\theta_\epsilon} - g^*)(x)| = \sup_{x \in D} |\partial^\alpha (g^{\theta_\epsilon} - g^*)(x)| \tag{A33}$$

By linearity of differentiation:

$$\sup_{x \in D} |\partial^\alpha g^{\theta_\epsilon}(x) - \partial^\alpha g^*(x)| < \epsilon \tag{A34}$$

The three inequalities in the corollary statement correspond to specific choices of α:

- For $\alpha = (0,0,0)$: $\sup_{x \in D} |g^{\theta_\epsilon}(x) - g^*(x)| < \epsilon$
- For $\alpha = (0,1,0)$: $\sup_{x \in D} |\partial_s g^{\theta_\epsilon}(x) - \partial_s g^*(x)| < \epsilon$
- For $\alpha = (0,2,0)$: $\sup_{x \in D} |\partial_s^2 g^{\theta_\epsilon}(x) - \partial_s^2 g^*(x)| < \epsilon$

Therefore, we have shown that convergence in the $W^{2,\infty}(D)$ norm implies uniform convergence of the function and its derivatives up to order 2. $\qquad\square$

Remark 1. *The choice of $W^{2,\infty}(D)$ is optimal as it:*

1. *Provides uniform control over derivatives needed for delta-gamma hedging*
2. *Ensures compactness properties necessary for approximation*
3. *Maintains compatibility with PDE regularity theory*

Hence, one obtains a sequence of neural networks g^{θ_ϵ} that converge uniformly to g^* and its first two spatial derivatives on D. This level of approximation fidelity is essential for implementing the subsequent hedging strategies that rely on accurate estimation of sensitivities.

$\square$

$\square$

Theorem 11 (Convergence under Self-Supervised Learning). *Let g^* be the unique solution to the no-arbitrage PDE with associated Greeks Δ_g and Γ_g. For the neural network g^θ trained with the delta-gamma hedging loss $\mathcal{L}_{\Delta,\Gamma}$, there exists a parameter vector θ^* achieving uniform approximation of both the solution and its derivatives.*

Proof. The proof proceeds in three steps.

1) Loss Function Analysis

Consider the delta-gamma hedging loss:

$$\mathcal{L}_{\Delta,\Gamma}(\theta) = \mathbb{E}\left[\left(\partial_s g^\theta \, dS_t + r_t(g^\theta - \partial_s g^\theta S_t)dt - dg^\theta \right)^2 + \lambda(\partial_s^2 g^\theta - \Gamma_g)^2 \right] \tag{A35}$$

where $\lambda > 0$ is a weighting parameter.

Lemma 12 (Loss Convergence). *If $g^\theta \to g^*$, $\partial_s g^\theta \to \Delta_g$, and $\partial_s^2 g^\theta \to \Gamma_g$ uniformly, then $\mathcal{L}_{\Delta,\Gamma}(\theta) \to 0$.*

Proof. By the no-arbitrage principle, g^* satisfies:

$$dg^* = \Delta_g dS_t + r_t(g^* - \Delta_g S_t)dt \tag{A36}$$

Therefore, as $g^\theta \to g^*$ and $\partial_s g^\theta \to \Delta_g$ uniformly:

$$|\partial_s g^\theta dS_t + r_t(g^\theta - \partial_s g^\theta S_t)dt - dg^\theta| \to |dg^* - dg^\theta| = 0 \tag{A37}$$
$$|\partial_s^2 g^\theta - \Gamma_g| \to 0 \tag{A38}$$

Hence, $\mathcal{L}_{\Delta,\Gamma}(\theta) \to 0$. $\qquad\qquad\qquad\qquad\qquad\qquad\qquad\qquad\square$

2) Existence of Minimizing Sequence

By the universal approximation theorem in Sobolev spaces (proved in previous steps), for any $\epsilon > 0$, there exists a sequence $(\theta_n)_{n \in \mathbb{N}}$ such that:

$$|g^{\theta_n} - g^*|_{W^{2,\infty}(D)} < \frac{\epsilon}{n} \tag{A39}$$

Proposition 13 (Minimizing Sequence Properties). *The sequence $(\theta_n)_{n \in \mathbb{N}}$ satisfies:*

$$\mathcal{L}_{\Delta,\Gamma}(\theta_n) \to 0 \ as \ n \to \infty \tag{A40}$$

Proof of Minimizing Sequence Properties. Let $(\theta_n)_{n \in \mathbb{N}}$ be the sequence constructed earlier satisfying

$$\|g^{\theta_n} - g^*\|_{W^{2,\infty}(D)} < \frac{\epsilon}{n} \tag{A41}$$

Decomposition of the Loss Function
Recall that $\mathcal{L}_{\Delta,\Gamma}(\theta)$ can be decomposed as:

$$\mathcal{L}_{\Delta,\Gamma}(\theta) = \mathbb{E}[L_1(\theta) + \lambda L_2(\theta)] \tag{A42}$$

where

$$L_1(\theta) = (\partial_s g^\theta dS_t + r_t(g^\theta - \partial_s g^\theta S_t)dt - dg^\theta)^2 \tag{A43}$$
$$L_2(\theta) = (\partial_s^2 g^\theta - \Gamma_g)^2 \tag{A44}$$

Convergence of $L_1(\theta_n)$
By the Sobolev embedding theorem and our assumption on θ_n:

$$\|g^{\theta_n} - g^*\|_{C^1(D)} \leq C_1 \|g^{\theta_n} - g^*\|_{W^{2,\infty}(D)} < \frac{C_1 \epsilon}{n} \tag{A45}$$

for some constant $C_1 > 0$. This implies:

$$|g^{\theta_n} - g^*| < \frac{C_1\epsilon}{n} \tag{A46}$$

$$|\partial_s g^{\theta_n} - \partial_s g^*| < \frac{C_1\epsilon}{n} \tag{A47}$$

Therefore:

$$|L_1(\theta_n)| \leq K_1 \left(\frac{\epsilon}{n}\right)^2 \tag{A48}$$

where K_1 depends on bounds for dS_t, r_t, and S_t.

Convergence of $L_2(\theta_n)$

Similarly, for the second derivative:

$$|\partial_s^2 g^{\theta_n} - \partial_s^2 g^*| < \frac{C_2\epsilon}{n} \tag{A49}$$

for some constant $C_2 > 0$. Therefore:

$$|L_2(\theta_n)| \leq K_2 \left(\frac{\epsilon}{n}\right)^2 \tag{A50}$$

Total Loss Convergence

Combining the bounds:

$$\mathcal{L}_{\Delta,\Gamma}(\theta_n) = \mathbb{E}[L_1(\theta_n) + \lambda L_2(\theta_n)] \tag{A51}$$

$$\leq (K_1 + \lambda K_2) \left(\frac{\epsilon}{n}\right)^2 \tag{A52}$$

$$\to 0 \text{ as } n \to \infty \tag{A53}$$

The convergence follows from the fact that ϵ is fixed while $n \to \infty$. $\square$

3) Convergence to Optimal Parameters

Theorem 14 (Existence of Optimal Parameters). *Given the compact parameter space Θ and continuous loss function $\mathcal{L}_{\Delta,\Gamma}$, there exists $\theta^* \in \Theta$ such that for any $\epsilon > 0$:*

$$\sup_{(t,s,h)\in D} |g^{\theta^*}(t,s,h) - g^*(t,s,h)| < \epsilon \tag{A54}$$

$$\sup_{(t,s,h)\in D} |\partial_s g^{\theta^*}(t,s,h) - \Delta_g(t,s,h)| < \epsilon \tag{A55}$$

$$\sup_{(t,s,h)\in D} |\partial_s^2 g^{\theta^*}(t,s,h) - \Gamma_g(t,s,h)| < \epsilon \tag{A56}$$

Proof. Let us establish the existence of optimal parameters and their approximation properties.

Construction of Minimizing Sequence:
By the previous proposition, there exists a sequence $(\theta_n)_{n \in \mathbb{N}}$ such that:

$$\mathcal{L}_{\Delta,\Gamma}(\theta_n) \to 0 \text{ as } n \to \infty \tag{A57}$$

Boundedness of Parameter Sequence:
Since Θ is compact, the sequence $(\theta_n)_{n \in \mathbb{N}}$ is bounded:

$$\|\theta_n\| \leq M \text{ for some } M > 0 \text{ and all } n \in \mathbb{N} \tag{A58}$$

Extraction of Convergent Subsequence:
By the Bolzano-Weierstrass theorem, since $(\theta_n)_{n \in \mathbb{N}}$ is bounded in the compact set Θ, there exists a convergent subsequence $(\theta_{n_k})_{k \in \mathbb{N}}$ and a limit point $\theta^* \in \Theta$ [37] such that:

$$\theta_{n_k} \to \theta^* \text{ as } k \to \infty \tag{A59}$$

Continuity Argument:
By the continuity of g^θ and its derivatives with respect to θ, for any $\delta > 0$, there exists $K > 0$ such that for all $k > K$:

$$\|g^{\theta_{n_k}} - g^{\theta^*}\|_{W^{2,\infty}(D)} < \frac{\epsilon}{3} \tag{A60}$$

$$\|g^{\theta_{n_k}} - g^*\|_{W^{2,\infty}(D)} < \frac{\epsilon}{3} \tag{A61}$$

Triangle Inequality:
Applying the triangle inequality:

$$\|g^{\theta^*} - g^*\|_{W^{2,\infty}(D)} \leq \|g^{\theta^*} - g^{\theta_{n_k}}\|_{W^{2,\infty}(D)} + \|g^{\theta_{n_k}} - g^*\|_{W^{2,\infty}(D)} \tag{A62}$$

$$< \frac{2\epsilon}{3} < \epsilon \tag{A63}$$

Component-wise Convergence:
The $W^{2,\infty}(D)$ norm bounds imply:

$$\sup_{(t,s,h) \in D} |g^{\theta^*}(t,s,h) - g^*(t,s,h)| \leq \|g^{\theta^*} - g^*\|_{W^{2,\infty}(D)} < \epsilon \tag{A64}$$

$$\sup_{(t,s,h) \in D} |\partial_s g^{\theta^*}(t,s,h) - \Delta_g(t,s,h)| \leq \|g^{\theta^*} - g^*\|_{W^{2,\infty}(D)} < \epsilon \tag{A65}$$

$$\sup_{(t,s,h) \in D} |\partial_s^2 g^{\theta^*}(t,s,h) - \Gamma_g(t,s,h)| \leq \|g^{\theta^*} - g^*\|_{W^{2,\infty}(D)} < \epsilon \tag{A66}$$

Optimality of θ^*:
By the continuity of $\mathcal{L}_{\Delta,\Gamma}$:

$$\mathcal{L}_{\Delta,\Gamma}(\theta^*) = \lim_{k \to \infty} \mathcal{L}_{\Delta,\Gamma}(\theta_{n_k}) = 0 \tag{A67}$$

41

Therefore, θ^* achieves the desired approximation properties. $\qquad\square$

Corollary 14.1 (Uniqueness and Stability). *The limit g^{θ^*} is unique and equals g^* by the uniqueness of the no-arbitrage PDE solution.*

Proof. We proceed by contradiction in several steps.

Assumption for Contradiction:

Suppose there exist two different limits $g^{\theta_1^*}$ and $g^{\theta_2^*}$ satisfying:

$$\mathcal{L}_{\Delta,\Gamma}(\theta_1^*) = \mathcal{L}_{\Delta,\Gamma}(\theta_2^*) = 0 \tag{A68}$$

No-Arbitrage PDE Analysis:

Both solutions must satisfy the no-arbitrage PDE:

$$\partial_t g + \frac{1}{2}\sigma^2 S^2 \partial_s^2 g + rS\partial_s g - rg = 0 \tag{A69}$$

with boundary condition:

$$g(T, s, h) = f(s, h) \tag{A70}$$

Property of Solutions:

For $i \in \{1, 2\}$:

$$\mathcal{L}_{\Delta,\Gamma}(\theta_i^*) = 0 \implies \partial_s g^{\theta_i^*} = \Delta_g \tag{A71}$$

$$\implies \partial_s^2 g^{\theta_i^*} = \Gamma_g \tag{A72}$$

Difference Analysis:

Let $w = g^{\theta_1^*} - g^{\theta_2^*}$. Then w satisfies:

$$\begin{cases} \partial_t w + \frac{1}{2}\sigma^2 S^2 \partial_s^2 w + rS\partial_s w - rw = 0 \\ w(T, s, h) = 0 \end{cases} \tag{A73}$$

Application of Maximum Principle:

By the classical maximum principle for parabolic PDEs (see [35]):

$$\sup_{(t,s,h)\in D} |w(t, s, h)| \leq \sup_{(s,h)\in\partial D} |w(T, s, h)| = 0 \tag{A74}$$

Therefore:

$$w(t, s, h) \equiv 0 \implies g^{\theta_1^*} = g^{\theta_2^*} \tag{A75}$$

Moreover, since g^* is the unique solution to the no-arbitrage PDE:

$$g^{\theta_1^*} = g^{\theta_2^*} = g^* \tag{A76}$$

The uniqueness of g^* from the PDE theory ensures that the only function achieving a vanishing residual and matching hedging constraints in the limit is g^*. Since

the loss is self-supervised—i.e., generated entirely by the PDE and the financial constraints—no other solution g^θ can yield zero residual unless it matches g^* and its derivatives exactly.

$\square$

Conclusion. We have shown that even without supervised labels, by using a self-supervised framework based on the PDE and hedging constraints, the neural network g^θ can approximate the unique solution g^* and its first two spatial derivatives. Given any $\epsilon > 0$, we can find θ^* such that:

$$\sup_{t, S_t, H_t} |g^{\theta^*}(S_t, H_t) - g^*(S_t, H_t)| < \epsilon, \quad |\Delta_{g^{\theta^*}} - \Delta_g| < \epsilon, \quad |\Gamma_{g^{\theta^*}} - \Gamma_g| < \epsilon.$$

Thus, the FINN model converges under delta-gamma hedging constraints in the self-supervised (unsupervised) learning setting.

$\square$

A.3 Geometric Brownian Motion Implementation

To demonstrate FINN's versatility in option pricing across different underlying asset models, we first tested our framework using the Geometric Brownian Motion (GBM) model. While FINN can accommodate various stochastic processes and empirical market data, GBM provides an ideal starting point due to its analytical tractability and widespread use in financial modeling. The GBM model describes asset price dynamics through the following stochastic differential equation:

$$dS(t) = \mu S(t)dt + \sigma S(t)dW(t) \tag{A77}$$

where μ represents the expected return (drift), σ denotes the asset's volatility, and $dW(t)$ represents the increment of a Wiener process, capturing random price fluctuations. For numerical implementation of GBM, we must transform the continuous-time stochastic differential equation into a discrete-time approximation suitable for computer simulation. We accomplish this using the Monte Carlo method with Euler-Maruyama discretization [38], a fundamental numerical scheme for approximating solutions to stochastic differential equations. Given a time step Δt, the discretized equation takes the form [38]:

$$S_{t+\Delta t} = S_t \exp\left((\mu - \frac{1}{2}\sigma^2)\Delta t + \sigma\sqrt{\Delta t}Z_t \right) \tag{A78}$$

This equation provides a method to calculate the asset price at the next time step ($S_{t+\Delta t}$) given the current price (S_t). The exponential form ensures that asset prices remain positive, which is a crucial property of stock prices. The equation A78 consists of two key components: a deterministic component $(\mu - \frac{1}{2}\sigma^2)\Delta t$ that adjusts for the drift (μ) of the process, with the $-(1/2)\sigma^2$ term serving as a necessary correction to ensure the expected return matches the continuous-time GBM model; and a random component $\sigma\sqrt{\Delta t}Z_t$, where Z_t represents a random draw from a standard normal distribution, with $\sqrt{\Delta t}$ scaling the random shock appropriately for the time step size and the volatility parameter σ determining the magnitude of these random fluctuations.

This discretization allows us to generate sample paths by iteratively computing price changes over small time intervals. For example, to simulate a price path over one year with daily steps, we would set $\Delta t = 1/252$ (assuming 252 trading days) and repeatedly apply this equation, drawing a new random normal variable Z_t at each step.

Under the assumptions of GBM, the Black-Scholes model provides analytical solutions for European option pricing. For a European call option C (which gives the right to buy) and a put option P (which gives the right to sell), the prices are given by:

$$
\begin{aligned}
C(S, K, t, T, \sigma, r) &= SN(d_1) - Ke^{-r(T-t)}N(d_2), \\
P(S, K, t, T, \sigma, r) &= Ke^{-r(T-t)}N(-d_2) - SN(-d_1),
\end{aligned} \tag{A79}
$$

These formulas incorporate several key parameters: the current stock price (S), strike price (K), current time (t), maturity time (T), volatility (σ), and risk-free rate (r).

The function $N(\cdot)$ represents the cumulative distribution function of the standard normal distribution. The terms d_1 and d_2 are defined as:

$$d_1 = \frac{\ln\left(\frac{S}{K}\right) + \left(r + \frac{\sigma^2}{2}\right)(T-t)}{\sigma\sqrt{T-t}}, \qquad d_2 = d_1 - \sigma\sqrt{T-t}. \qquad (A80)$$

To manage the risk associated with option positions, traders rely on hedge ratios, particularly Delta (Δ). Delta measures the rate of change in the option price with respect to changes in the underlying asset price, mathematically expressed as:

$$\Delta_{\text{call}} = \frac{\partial C}{\partial S}, \Delta_{\text{put}} = \frac{\partial P}{\partial S} \qquad (A81)$$

To rigorously evaluate our FINN model's performance, we conduct extensive testing using thousands of simulated scenarios. We compare FINN's predictions against these Black-Scholes analytical solutions using two comprehensive metrics: Mean Absolute Deviation (MAD) and Mean Square Error (MSE). These metrics assess both the accuracy of option prices and hedge ratios. This systematic evaluation framework enables us to verify FINN's capability to learn and reproduce the fundamental pricing relationships that the Black-Scholes model captures mathematically.

A.4 The Heston Stochastic Volatility Implementation

The Heston stochastic volatility model [39] addresses fundamental limitations of the Black-Scholes framework by incorporating time-varying volatility dynamics. This extension enables the model to capture empirically observed market phenomena, particularly the non-constant nature of asset price volatility and the leverage effect—the negative correlation between asset returns and volatility changes. By allowing volatility to evolve according to its own stochastic process, the Heston model provides a more sophisticated mathematical framework for option pricing that aligns with observed market behavior.

In this model, both the asset price and its volatility evolve according to coupled stochastic processes. The asset price S_t follows the process:

$$dS_t = \mu S_t dt + \sqrt{\nu_t} S_t dW_t^S \qquad (A82)$$

What makes this model special is that the volatility itself ($\sqrt{\nu_t}$) follows an Ornstein-Uhlenbeck process:

$$d\sqrt{\nu_t} = -\theta\sqrt{\nu_t}dt + \xi dW^\nu \qquad (A83)$$

Through application of Itô's lemma, we can show that the variance ν_t follows a Cox-Ingersoll-Ross (CIR) process [40]:

$$d\nu_t = \kappa(\theta - \nu_t)dt + \xi\sqrt{\nu_t}dW_t^\nu \qquad (A84)$$

The two Wiener processes W_t^S and W_t^ν are correlated with correlation coefficient ρ, allowing the model to capture the leverage effect observed in equity markets.

$$dW_t^S dW_t^\nu = \rho dt \tag{A85}$$

This equation shows how the two Brownian motions are correlated, with $\rho = -0.7$ in our implementation. This negative correlation captures the leverage effect: when asset prices decrease, volatility tends to increase, and vice versa.

Overall, the Heston model is characterized by five key parameters:

- Initial variance (ν_0): The starting point for the variance process
- Long-term variance (θ): The level around which the variance tends to oscillate
- Mean reversion rate (κ): How quickly the variance returns to its long-term average
- Volatility of volatility (ξ): How much the variance itself fluctuates (volvol)
- Correlation (ρ): Between asset returns and variance changes

To ensure the variance remains positive, the parameters must satisfy [41]:

$$2\kappa\theta > \xi^2 \tag{A86}$$

Under risk-neutral pricing, the European call option value is:

$$C_0 = S_0 \cdot \Pi_1 - e^{-rT} K \cdot \Pi_2 \tag{A87}$$

where Π_1 and Π_2 are risk-neutral probabilities computed through characteristic functions:

$$
\begin{aligned}
\Pi_1 &= \frac{1}{2} + \frac{1}{\pi} \int_0^\infty \mathrm{Re}\left[\frac{e^{-i \cdot w \cdot \ln(K)} \cdot \Psi_{\ln S T}(w - i)}{i \cdot w \cdot \Psi \ln S\, T(-i)} \right] dw \\
\Pi_2 &= \frac{1}{2} + \frac{1}{\pi} \int_0^\infty \mathrm{Re}\left[\frac{e^{-i \cdot w \cdot \ln(K)} \cdot \Psi \ln S_T(w)}{i \cdot w} \right] dw
\end{aligned}
\tag{A88}
$$

The option price in the Heston model requires computing a characteristic function Ψ, which encapsulates the probabilistic behavior of future asset prices under stochastic volatility. This characteristic function is constructed using several interrelated auxiliary functions, each playing a specific role in capturing different aspects of the model's dynamics. The complete expression for the characteristic function takes the form [39]:

$$\Psi_{lnS_T}(w) = e^{\left[C(t,w)\cdot\theta + D(t,w)\cdot\nu_0 + i\cdot w\cdot\ln\left(S_0 \cdot e^{rt}\right) \right]} \tag{A89}$$

where $C(t, w)$ captures the long-term variance effects, $D(t, w)$ incorporates the current variance level, and the exponential term with $\ln(S_0 \cdot e^{rt})$ accounts for the deterministic drift in asset prices.

In our experimental implementation, we used carefully chosen parameters that reflect typical market conditions:

$$r = 0, \qquad\qquad\qquad\qquad \text{\# interest rate}$$

$$dt = \frac{1}{250}, \qquad\qquad\qquad\quad \text{\# Euler Discretization Period}$$

$$\xi = [0.125, 0.15, 0.175], \qquad \text{\# vol of vol}$$

$$\rho = -0.7, \qquad\qquad\qquad\quad \text{\# correlation of two brownian motions}$$

$$\kappa = 1.25, \qquad\qquad\qquad\quad \text{\# mean-reversion parameter}$$

$$\theta = 0.0225, \qquad\qquad\qquad \text{\# long term average variance, Theta}$$

$$\nu_0 = 0.0225 \qquad\qquad\qquad \text{\# initial variance}$$

These parameter choices ensure realistic market dynamics while maintaining numerical stability in our simulations.

A.5   GBM European Put Results

Here we present the results and summary statistics of running the FINN on the put options:
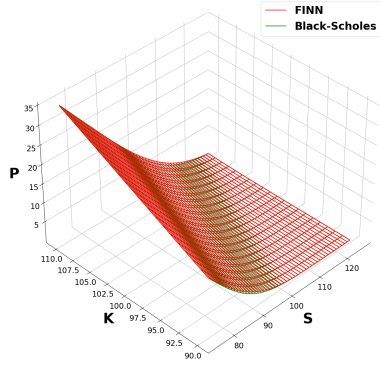
(a) Estimated Put Option Price for Given S and K
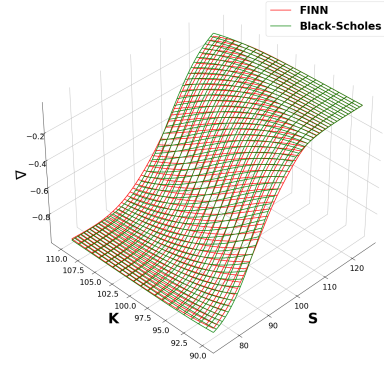
(b) Estimated Hedge Ratio (Δ) Given S and K
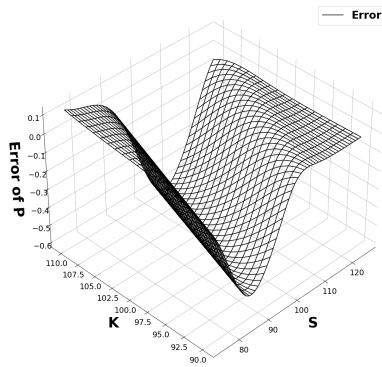
(c) Error of Predicted Put Price
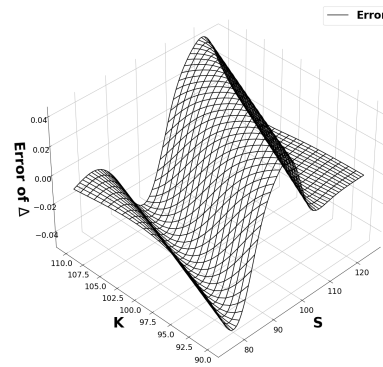
(d) Error of Predicted Hedge Ratio (Δ)

Fig. A1: Comparison of Put Option Prices, Hedge Ratios, and Errors (GBM)

Table A1: FINN Testing Results on Various Volatility Levels, TTMs, and Strikes (GBM) for Put Options. Results are averaged across strikes from 75 to 125, based on 10,000 data points, with the final values being averaged over 10 independent runs, the values in bracket are the standard deviation.

| Vol σ	TTM τ	Put Option Price (P) Estimation				Hedge Ratio (Δ) Estimation			
		MAD		MSE		MAD		MSE	
	0.24	0.160	(0.045)	0.059	(0.033)	0.020	(0.006)	0.001	(0.001)
	0.28	0.173	(0.049)	0.066	(0.038)	0.021	(0.006)	0.001	(0.001)
	0.32	0.183	(0.053)	0.072	(0.041)	0.021	(0.006)	0.001	(0.000)
0.125	0.36	0.190	(0.057)	0.076	(0.044)	0.021	(0.006)	0.001	(0.000)
	0.40	0.195	(0.061)	0.079	(0.047)	0.021	(0.006)	0.001	(0.000)
	0.44	0.199	(0.064)	0.080	(0.049)	0.021	(0.006)	0.001	(0.000)
	0.48	0.201	(0.067)	0.081	(0.050)	0.021	(0.006)	0.001	(0.000)
	0.24	0.237	(0.064)	0.108	(0.047)	0.024	(0.004)	0.001	(0.000)
	0.28	0.254	(0.066)	0.120	(0.050)	0.025	(0.004)	0.001	(0.000)
	0.32	0.267	(0.068)	0.131	(0.053)	0.025	(0.004)	0.001	(0.000)
0.15	0.36	0.279	(0.069)	0.139	(0.057)	0.026	(0.004)	0.001	(0.000)
	0.40	0.288	(0.070)	0.146	(0.060)	0.026	(0.004)	0.001	(0.000)
	0.44	0.295	(0.072)	0.150	(0.063)	0.025	(0.005)	0.001	(0.000)
	0.48	0.300	(0.073)	0.151	(0.066)	0.025	(0.005)	0.001	(0.000)
	0.24	0.293	(0.067)	0.150	(0.068)	0.026	(0.006)	0.001	(0.000)
	0.28	0.313	(0.074)	0.166	(0.077)	0.027	(0.006)	0.001	(0.000)
	0.32	0.327	(0.080)	0.177	(0.084)	0.027	(0.006)	0.001	(0.000)
0.175	0.36	0.338	(0.084)	0.184	(0.089)	0.027	(0.006)	0.001	(0.000)
	0.40	0.345	(0.089)	0.188	(0.093)	0.026	(0.006)	0.001	(0.000)
	0.44	0.350	(0.093)	0.190	(0.096)	0.026	(0.006)	0.001	(0.000)
	0.48	0.353	(0.098)	0.189	(0.099)	0.025	(0.006)	0.001	(0.000)

A.6 Heston European Put Results
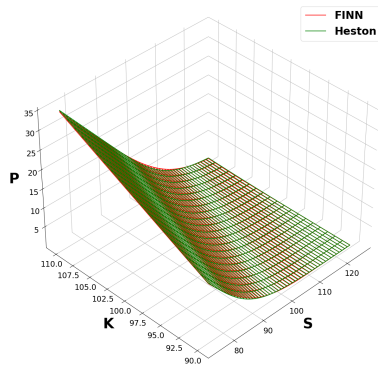
(a) Estimated Put Option Price for Given S and K (Heston)
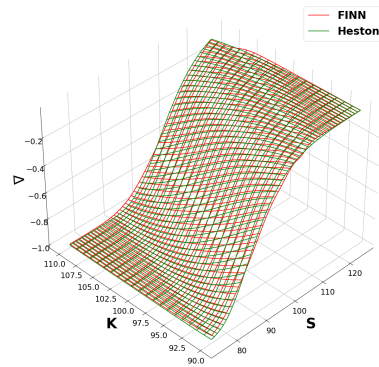
(b) Estimated Hedge Ratio (Δ) Given S and K (Heston)
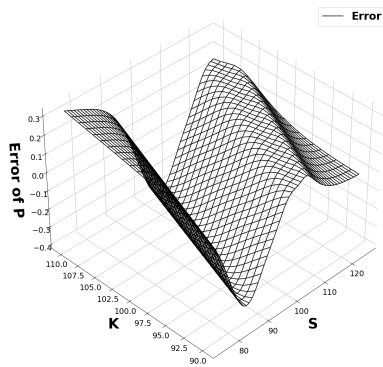
(c) Error of Predicted Put Price (Heston)
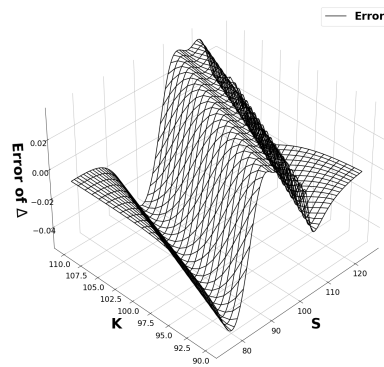
(d) Error of Predicted Hedge Ratio (Δ) (Heston)

Fig. A2: Comparison of Put Option Prices, Hedge Ratios, and Errors (Heston Model)

Table A2: FINN Testing Results on Various Volatility Levels, TTMs, and Strikes (Heston) for Put Options. Results are averaged across strikes from 75 to 125, based on 10,000 data points, with the final values being averaged over 10 independent runs, the values in bracket are the standard deviation.

VolVol ξ	TTM τ	Put Option Price (P) Estimation MAD		MSE		Hedge Ratio (Δ) Estimation MAD		MSE	
	0.24	0.217	(0.127)	0.117	(0.109)	0.024	(0.011)	0.001	(0.001)
	0.28	0.242	(0.138)	0.137	(0.127)	0.026	(0.012)	0.001	(0.001)
	0.32	0.263	(0.147)	0.155	(0.142)	0.027	(0.012)	0.001	(0.001)
0.125	0.36	0.282	(0.153)	0.170	(0.153)	0.028	(0.012)	0.001	(0.001)
	0.40	0.299	(0.157)	0.184	(0.163)	0.029	(0.012)	0.001	(0.001)
	0.44	0.314	(0.160)	0.197	(0.171)	0.029	(0.011)	0.001	(0.001)
	0.48	0.329	(0.161)	0.210	(0.179)	0.030	(0.011)	0.001	(0.001)
	0.24	0.218	(0.132)	0.119	(0.130)	0.027	(0.011)	0.001	(0.001)
	0.28	0.241	(0.141)	0.139	(0.149)	0.028	(0.011)	0.001	(0.001)
	0.32	0.261	(0.148)	0.156	(0.166)	0.029	(0.012)	0.001	(0.001)
0.15	0.36	0.280	(0.154)	0.173	(0.181)	0.030	(0.012)	0.001	(0.001)
	0.40	0.298	(0.159)	0.189	(0.194)	0.031	(0.012)	0.002	(0.001)
	0.44	0.316	(0.164)	0.204	(0.207)	0.032	(0.012)	0.002	(0.001)
	0.48	0.333	(0.168)	0.219	(0.217)	0.032	(0.012)	0.002	(0.001)
	0.24	0.239	(0.131)	0.139	(0.141)	0.029	(0.010)	0.002	(0.001)
	0.28	0.265	(0.140)	0.163	(0.163)	0.031	(0.011)	0.002	(0.001)
	0.32	0.288	(0.147)	0.184	(0.181)	0.033	(0.011)	0.002	(0.001)
0.175	0.36	0.309	(0.153)	0.204	(0.198)	0.034	(0.011)	0.002	(0.001)
	0.40	0.329	(0.157)	0.224	(0.212)	0.035	(0.012)	0.002	(0.001)
	0.44	0.349	(0.161)	0.243	(0.225)	0.036	(0.011)	0.002	(0.001)
	0.48	0.369	(0.164)	0.263	(0.236)	0.037	(0.011)	0.002	(0.001)

A.7 FINN Delta-Gamma Hedging Results on Various Volatility Levels

Table A3: FINN Delta-Gamma Hedging Results on Various Volatility Levels, TTMs, and Strikes for Call Options (GBM). Results are averaged across strikes from 75 to 125, based on 10,000 data points, with the final values being averaged over 10 independent runs, the values in bracket are the standard deviation.

Vol σ	Hedging Option TTM τ_{hedge}	Option TTM τ	Call Option Price (C) Estimation MAD		MSE		Hedge Ratio (Δ) Estimation MAD		MSE		Option Gamma (Γ) Estimation MAD		MSE	
0.125	0.12	0.24	0.024	(0.010)	0.001	(0.001)	0.004	(0.001)	0.0	(0.0)	0.001	(0.0)	0.0	(0.0)
		0.28	0.023	(0.011)	0.001	(0.001)	0.004	(0.001)	0.0	(0.0)	0.001	(0.0)	0.0	(0.0)
		0.32	0.023	(0.012)	0.001	(0.001)	0.004	(0.001)	0.0	(0.0)	0.001	(0.0)	0.0	(0.0)
		0.36	0.024	(0.012)	0.001	(0.001)	0.004	(0.001)	0.0	(0.0)	0.001	(0.0)	0.0	(0.0)
		0.40	0.026	(0.013)	0.001	(0.002)	0.004	(0.001)	0.0	(0.0)	0.001	(0.0)	0.0	(0.0)
		0.44	0.028	(0.015)	0.001	(0.002)	0.004	(0.001)	0.0	(0.0)	0.001	(0.0)	0.0	(0.0)
		0.48	0.030	(0.016)	0.002	(0.002)	0.004	(0.001)	0.0	(0.0)	0.001	(0.0)	0.0	(0.0)
	0.36	0.24	0.023	(0.019)	0.001	(0.002)	0.003	(0.001)	0.0	(0.0)	0.001	(0.0)	0.0	(0.0)
		0.28	0.024	(0.021)	0.002	(0.003)	0.003	(0.001)	0.0	(0.0)	0.001	(0.0)	0.0	(0.0)
		0.32	0.026	(0.022)	0.002	(0.004)	0.003	(0.001)	0.0	(0.0)	0.001	(0.0)	0.0	(0.0)
		0.36	0.028	(0.024)	0.002	(0.004)	0.003	(0.001)	0.0	(0.0)	0.001	(0.0)	0.0	(0.0)
		0.40	0.030	(0.026)	0.002	(0.005)	0.003	(0.001)	0.0	(0.0)	0.001	(0.0)	0.0	(0.0)
		0.44	0.033	(0.028)	0.003	(0.005)	0.003	(0.001)	0.0	(0.0)	0.001	(0.0)	0.0	(0.0)
		0.48	0.035	(0.030)	0.003	(0.006)	0.003	(0.001)	0.0	(0.0)	0.001	(0.0)	0.0	(0.0)
0.15	0.12	0.24	0.023	(0.014)	0.001	(0.001)	0.003	(0.001)	0.0	(0.0)	0.001	(0.0)	0.0	(0.0)
		0.28	0.023	(0.013)	0.001	(0.001)	0.003	(0.001)	0.0	(0.0)	0.001	(0.0)	0.0	(0.0)
		0.32	0.024	(0.011)	0.001	(0.001)	0.003	(0.001)	0.0	(0.0)	0.001	(0.0)	0.0	(0.0)
		0.36	0.024	(0.010)	0.001	(0.001)	0.003	(0.001)	0.0	(0.0)	0.001	(0.0)	0.0	(0.0)
		0.40	0.025	(0.009)	0.001	(0.001)	0.003	(0.001)	0.0	(0.0)	0.001	(0.0)	0.0	(0.0)
		0.44	0.026	(0.009)	0.001	(0.001)	0.003	(0.001)	0.0	(0.0)	0.001	(0.0)	0.0	(0.0)
		0.48	0.027	(0.010)	0.001	(0.001)	0.003	(0.001)	0.0	(0.0)	0.001	(0.0)	0.0	(0.0)
	0.36	0.24	0.029	(0.021)	0.002	(0.003)	0.003	(0.001)	0.0	(0.0)	0.001	(0.0)	0.0	(0.0)
		0.28	0.028	(0.020)	0.002	(0.003)	0.002	(0.001)	0.0	(0.0)	0.001	(0.0)	0.0	(0.0)
		0.32	0.028	(0.020)	0.002	(0.003)	0.002	(0.001)	0.0	(0.0)	0.001	(0.0)	0.0	(0.0)
		0.36	0.030	(0.020)	0.002	(0.003)	0.002	(0.001)	0.0	(0.0)	0.001	(0.0)	0.0	(0.0)
		0.40	0.032	(0.021)	0.002	(0.003)	0.002	(0.001)	0.0	(0.0)	0.001	(0.0)	0.0	(0.0)
		0.44	0.034	(0.023)	0.003	(0.003)	0.002	(0.001)	0.0	(0.0)	0.001	(0.0)	0.0	(0.0)
		0.48	0.037	(0.025)	0.003	(0.004)	0.002	(0.001)	0.0	(0.0)	0.001	(0.0)	0.0	(0.0)
0.175	0.12	0.24	0.027	(0.017)	0.001	(0.001)	0.003	(0.002)	0.0	(0.0)	0.001	(0.0)	0.0	(0.0)
		0.28	0.028	(0.018)	0.001	(0.001)	0.002	(0.002)	0.0	(0.0)	0.001	(0.0)	0.0	(0.0)
		0.32	0.029	(0.019)	0.001	(0.001)	0.002	(0.002)	0.0	(0.0)	0.001	(0.0)	0.0	(0.0)
		0.36	0.030	(0.021)	0.002	(0.001)	0.002	(0.002)	0.0	(0.0)	0.001	(0.0)	0.0	(0.0)
		0.40	0.030	(0.022)	0.002	(0.002)	0.002	(0.002)	0.0	(0.0)	0.001	(0.0)	0.0	(0.0)
		0.44	0.030	(0.023)	0.002	(0.002)	0.002	(0.002)	0.0	(0.0)	0.0	(0.0)	0.0	(0.0)
		0.48	0.030	(0.024)	0.002	(0.002)	0.002	(0.002)	0.0	(0.0)	0.0	(0.0)	0.0	(0.0)
	0.36	0.24	0.019	(0.017)	0.001	(0.003)	0.003	(0.002)	0.0	(0.0)	0.001	(0.0)	0.0	(0.0)
		0.28	0.021	(0.018)	0.001	(0.003)	0.002	(0.002)	0.0	(0.0)	0.001	(0.0)	0.0	(0.0)
		0.32	0.022	(0.019)	0.001	(0.003)	0.002	(0.002)	0.0	(0.0)	0.001	(0.0)	0.0	(0.0)
		0.36	0.023	(0.021)	0.002	(0.003)	0.002	(0.002)	0.0	(0.0)	0.001	(0.0)	0.0	(0.0)
		0.40	0.024	(0.022)	0.002	(0.003)	0.002	(0.002)	0.0	(0.0)	0.001	(0.0)	0.0	(0.0)
		0.44	0.024	(0.023)	0.002	(0.004)	0.002	(0.002)	0.0	(0.0)	0.001	(0.0)	0.0	(0.0)
		0.48	0.025	(0.024)	0.002	(0.004)	0.002	(0.002)	0.0	(0.0)	0.0	(0.0)	0.0	(0.0)